MUT/2019/11

COMMITTEE ON THE MUTAGENICITY OF CHEMICALS IN FOOD CONSUMER PRODUCTS AND THE ENVIRONMENT

REVIEW OF GENOTOXICITY OF PATULIN (PAT)

Referral to COM

1. The Food Standards Agency (FSA) has asked for advice on the genotoxicity of PAT to assist in developing advice for risk assessment requests for food products contaminated with PAT.

2. A Committee on Toxicity of Chemicals in Food, Consumer Products and the Environment (COT) paper on review of potential risks from PAT in the diet of infants aged 0 to 12 months and children aged 1 to 5 years (TOX/2019/19) was presented in May 2019. The genotoxicity data was variable and therefore the COT are requesting that the COM review it.

3. Regarding previous assessment on the carcinogenicity of PAT, the International Agency for Research on Cancer classified PAT in group 3, since the evidence of carcinogenicity was considered limited in experimental animal (International Agency for Research on Cancer, 1986[1]). This has been restated in a factsheet by the WHO last year which states that: “Patulin is considered to be genotoxic however a carcinogenic potential has not been demonstrated”[2].

Introduction

4. The Scientific Advisory Committee on Nutrition (SACN) is undertaking a review of scientific evidence that will inform the Government’s dietary recommendations for infants and young children aged up to 5 years. The SACN is examining the nutritional basis of the advice. The Committee on Toxicity of Chemicals in Food, Consumer Products and the Environment (COT) was asked to review the risks of toxicity from chemicals in the diet of infants, which has been completed, and young children. The reviews will identify new evidence that has emerged since the Government’s recommendations were formulated and will appraise that evidence to determine whether the advice should be revised.

5. PAT is a mycotoxin produced by certain species of the genera *Aspergillus* and *Penicillium*, including *A. clavatus*, *P. expansum*, *P. patulum*, *P. aspergillus* and *P. byssochlamys*. *P. expansum* is a common spoilage microorganism in apples. The major potential dietary sources of patulin are apples and apple juice made from affected fruit (FAO/WHO, 1995). Since 1995, PAT has been frequently found in apples, pears, their juices and jams and other products derived from these fruits (Kawashima *et al*., 2002). It has also been detected in other fruits, like grapes,

[1] http://www.inchem.org/documents/iarc/vol40/patulin.html
[2] https://www.who.int/news-room/fact-sheets/detail/mycotoxins

cherries, plums, blueberries, oranges, strawberries and melons (Frank, 1977; Bartolomé, 1994; Li *et al*., 2007).

6. A scoping paper (TOX/2015/32[3]) "COT contribution to SACN review of complementary and young child feeding; proposed scope of work for 1-5 year old children" was reviewed by the COT in 2015. A further scoping paper for mycotoxins was presented to the COT in 2017[4].

7. The most recent evaluation of PAT was conducted by the Joint FAO/WHO Expert Committee on Food Additives (JECFA) (FAO/WHO, 1995[5]). Prior to that, JECFA evaluated PAT in 1990. In this evaluation, JECFA established a provisional maximum tolerable weekly intake (PMTWI) of 7 µg/kg bodyweight (bw) (FAO/WHO, 1990). The Scientific Committee on Food (SCF), in 1994 agreed with the PTWI of 7 µg/kg bw established by JECFA, in 1990 (SCF, 1994). In 2000, the SCF produced a minute statement[6] and endorsed the provisional maximum tolerable daily intake (PMTDI) of 0.4 µg/kg bw established by JECFA in 1995 (SCF, 2000).

8. The recent review of potential risks from PAT in the diet of infants aged 0 to 12 months and children aged 1 to 5 years was presented in May 2019 and the COT concluded that the new toxicological data (excluding the new genotoxicity data) between 1995-2018 would not change the health-based guidance (HBGV) value. The COT is requesting that the COM review the genotoxicity data before a final conclusion on the risks of PAT can be made.

Structure, reactivity and stability

9. PAT has a chemical formula of $C_7H_6O_4$ and a molar mass of 154.12 g/mol.

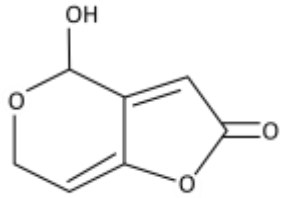

Figure 1. Chemical structure of patulin

10. PAT is an organic compound that is classified as a polyketide[7]. It is stable in low pH media and resistant to thermal denaturation. PAT was reported to promptly react with sulfur dioxide (SO_2), so it could be destroyed when an antioxidant or antimicrobial agent containing SO_2 is used (Roland and Beuchat, 1984). The fortification with ascorbic acid also showed to be an efficient method to reduce the levels of the toxin (Brackett & Marth, 1979; Drusch *et al*., 2007), as well as the addition of thiamine, pyridoxine and calcium pantotenate (Yazici & Velioglu, 2002).

[3] https://cot.food.gov.uk/sites/default/files/tox2017-15.pdf
[4] https://cot.food.gov.uk/sites/default/files/tox2017-30_0.pdf
[5] https://apps.who.int/iris/bitstream/handle/10665/37246/WHO_TRS_859.pdf;jsessionid=98CAFC5CB9D10C9C7BA763B1B89BDE5F?sequence=1
[6] https://ec.europa.eu/food/sites/food/files/safety/docs/cs_contaminants_catalogue_patulin_out55_en.pdf
[7] Polyketides are a large group of secondary metabolites which either contain alternating carbonyl and methylene groups (-CO-CH2-), or are derived from precursors which contain such alternating groups. Many polyketides have antimicrobial and immunosuppressive properties. Many mycotoxins produced by fungi are polyketides.

Adsorption, Distribution, Metabolism and Excretion Summary

11. From past *in vivo* experimental studies, it was concluded that the major retention sites of PAT are erythrocytes and blood-rich organs (spleen, kidney, lung and liver) (Dailey *et al*., 1977). From the Dailey *et al.* study, 17 male and 12 female adult rats were given a single oral dose of [^{14}C] PAT and were sacrificed at various time intervals from 4 hours to 7 days following administration of the PAT. Two groups of rats were employed; the treated group had been exposed to daily oral doses of unlabelled patulin (dissolved in pH 5.0 citrate buffer) in utero and for 41–66 weeks after weaning, while the controls were given the buffer only throughout gestation and for 38–81 weeks after weaning. Approximately 49% of the administered ^{14}C radioactivity was recovered from faeces and 36% from urine within 7 days after dosing. Most of the excretion of labelled material occurred within the first 24 hours. All of the ^{14}C activity detected in the urine samples was either metabolites or the original [^{14}C] patulin. About 1–2% of the total radioactivity was recovered as $^{14}CO_2$ from expired air. Carbon-14 radioactivity in various tissues and organs was determined throughout the 7 day period; the most significant retention site was the red blood cells (Dailey *et al.*, 1977).

Mode of action summary

12. PAT has a strong affinity for sulfhydryl groups which in turn may inhibit enzyme activity (Puel *et al*., 2010). In several studies, it has been concluded that the presence of reactive oxygen species (ROS) and depletion of intracellular glutathione (GSH) is key for PAT mediated toxicity and in turn the main mode of action via inducing oxidative damage (Barhoumi *et al*., 1996., Burghardt *et al*., 1992, Guo *et al*., 2013, Ianiri *et al*., 2016).

Toxicity Summary

13. The oral lethal dose (LD_{50}[8]) value of PAT in mice and rats varies from 20–100 mg/kg bw (Pal *et al*., 2017).

14. The intravenous and intraperitoneal routes are more toxic than the oral route (Pal *et al*., 2017).

15. Acute studies have shown that PAT causes haemorrhages, formation of oedema and dilation of the intestinal tract in experimental animals (McKinley *et al*., 1982). In subchronic studies, hyperaemia of the duodenal epithelium and kidney function impairment were observed as the main effects (McKinley *et al*., 1980).

16. Toxicological data published between 1995 and 2018 reconfirms that dietary exposure of PAT leads to systemic toxicity in the mammalian system including intestinal injury, intestinal ulcers, inflammation, bleeding and a decrease in transepithelial resistance. PAT causes liver inflammation (inducing a rise in alanine aminotransferase (ALT), aspartate transaminase (AST) and malondialdehyde (MDA)). PAT also causes detrimental effects on other target organs such as kidneys and the thyroid. Cellular and genetic material affects include DNA strand breaks,

[8] LD_{50}: lethal dose at which 50 % of the test population is dead.

neuronal degeneration, and degeneration of glomeruli and renal tubules (Song *et al*., 2014; Mohan *et al*., 2012; Ayed-Boussema *et al*., 2012; Maidana *et al*., 2016; Puel *et al*., 2010; Al-Hazmi, 2010; de Melo *et al*., 2012).

Genotoxicity of PAT

In vitro

Bacteria

17. PAT caused DNA single-strand breaks in living cells of *Escherichia coli* using analysis of DNA by alkaline and neutral sucrose gradient centrifugation (Lee, K.S. and Röschenthaler 1986).

18. The bacterial strains used were as follows: *E. coli* D110, *polA endA* Thy-, *E. coli* X8011, F- Δ*lac-169* B1-(λ *c*I857 h80 d*lac*) (λ *c*I857 h80), *E. coli* MRE600, *E. coli* X8011 strain (used as an indicator). Two isogenic strains were designated as *E. coli* X8011(λ) and *E. coli* X 8011λ -.The lysogenic *Bacillus megaterium* strain NRRL-B 6395 and its indicator strain NRRL-B 6394 were grown in TGY medium (Whittaker and Chipley 1979).

19. For experiments with alkaline and neutral sucrose gradient analysis, M9 medium (Adams, 1959) was supplemented with thymine (20 µg/ml) for *E. coli* D110. The induction of prophages in *E. coli* X8011 was carried out in 2YT medium (Miller, 1972). The plaque tests were done according to the double-layer technique of Adams *et al* 1959 with diagnostic sensitivity test agar as bottom agar and 0.6% soft agar. Bacteria for the preparation of permeabilized cells were grown in M3 medium. The analysis of single-strand breaks in bacteria treated with 10 µg, 20 µg and 50 µg of PAT per ml for 60 minutes was performed according to the method of McGrath and Williams (1966) by radioactive labelling of the bacterial DNA, preparation of protoplasts, and lysis on 5 to 20% alkaline sucrose gradients (pH 12). Centrifugation was done at 100, 000 x g for 2 hours in an ultracentrifuge. After fractionation of the gradients the radioactivity of the trichloroacetic acid-precipitable material was counted on fiber glass filters. The results are presented as percentage of radioactivity in each fraction of the total acid-precipitable radioactivity. Samples not treated with PAT were the negative control, the positive control samples without patulin were irradiated before analysis with UV_{254} (1.2 J m^{-2} s^{-1}) for 30 or 60 s as indicated. Neutral sucrose gradients were performed entirely by the method of Krasin and Hutchinson (1977). They were run for 1 hour at 100, 000 x g. For investigation of *in vivo* DNA repair in the presence of 10 µg of PAT per ml, the bacteria were washed and irradiated with UV_{254} in an M9-salts solution containing 20 µg of thymine per ml and 37 mM $MgSO_4$. The irradiated bacteria were incubated in the presence of PAT at 37°C in the dark. Samples were withdrawn at different times and analyzed by the alkaline sucrose gradient technique.

20. For the induction of lysogenic bacteria, a prophage λ *c*1857*ts* induction test similar to that of Ho and Ho (1981) was used[9]. PAT was not treated with an S-9 liver fraction for metabolic activation. The lysis of patulin-, UV_{254}-, and temperature-induced cultures of *E. coli* X8011(λ) was checked by optical density measurements at 546 nm. The ratio of phage counts from patulin-treated cells (T) to phage counts from control cells (C) was calculated according to HIeinemann (1971) except that the phage counts per millilitre were related to the cell counts per milliliter as determined with a Helber chamber. This was done because the control culture of *E. coli* X8011(λ), having a constant spontaneous induction rate yielding 1 plaque per 5 x 10^5 cells, would exceed the number of bacterial cells in the PAT-inhibited culture by several orders of magnitude. The T/C ratio gave a pessimistic estimate of how many more phages per cell were produced in the treated culture compared with the control.

21. Permeabilized cells were either toluenized cells obtained according to the procedures of Moses and Richardson (1970) and Staudenbauer (1976) or plasmolyzed cells by the method of Ben-Hamida and Gros (1971). Both systems allowed for distinction of replicative DNA synthesis from DNA repair synthesis. The replicative synthesis occurred in the presence of the four deoxyribonucleotide triphosphates (0.02 mM), ATP (2 mM), and NAD (0.1 mM), whereas the repair synthesis required no ATP and NAD. The addition of DNase I or PAT to the cells and a PolA+ strain (*E. coli* MRE600) were necessary for the demonstration of repair. Protein synthesis occurred in plasmolyzed cells only. It was dependent on the four ribonucleotide triphosphates (0.5 mM) and on the 20 amino acids (0.25 mM), phosphoenolpyruvate, and phosphoenolpyruvate kinase. In plasmolyzed cells mRNA synthesis can be distinguished from synthesis of stable RNAs as the latter only occurs in the presence of protein synthesis. For the measurements one of the nucleotides or amino acids was always replaced by a radioactive one, and the incorporation of radioactivity into acid-precipitable material was measured in a liquid scintillation counter after precipitation with trichloroacetic acid on glass-fiber filters.

22. It was demonstrated that at a concentration of 10 µg/ml for 60 min, PAT caused DNA single-strand breaks in living cells of *Escherichia coli*. At 50 µg/ml, double-strand breaks were also observed. The sedimentation profiles of the chromosomal DNA of repair-deficient (polA) *E. coli* D110 cells in alkaline sucrose gradients indicated single-strand breaks of DNA when the cells had been treated with 10 or 20 µg of patulin per ml. The shift towards smaller DNA fragments was more pronounced with the higher concentration (Fig. 1B). At doses of 50 µg/ml, double-strand breaks could be demonstrated in neutral sucrose gradients (Fig. 1D). The authors stated that DNA-damaging activity of PAT was dose dependent.
It was noted that single-strand breaks were induced by UV_{254} irradiation of *E. coli* MRE600 cells. Fig 2B shows the sedimentation profiles after repair incubation of the cells in M9 solution without a carbon source at 37°C for 90 min. At this time the DNA repair was as complete as that of the control without PAT. Thus, no irreversible inhibition of DNA repair occurred.

23. In addition, the authors reported the induction of prophage in lysogenic bacteria. *E. coli* cells lysogenic for the wild-type lambda phage could not be induced

[9] with the exception that the host was not an *E. coli envA uvrB* mutant but *E. coli* X8011(λ) and the plaque-counting technique with *E. coli* X8011 λ - as indicator for the estimation of liberated phage was used

by PAT. However, *E. coli* X8011(λ), a temperature-sensitive, double lysogenic strain was induced by PAT when incubated at 35°C, a temperature below the inducing temperature. This strain lysed with 10 µg of patulin per ml, whereas the isogenic strain *E. coli* X8011λ- showed only growth inhibition at the same concentration. Virtually the same curve was obtained when in addition to 10 µg of PAT per ml, 20 µg of cysteine per ml was added to *E. coli* X8011(λ), indicating inactivation of PAT by cysteine. Quite similar results were obtained with the *B. megaterium strain* used previously by Whittaker and Chipley (1979) for testing prophage inducibility by aflatoxin B1.

24. High concentrations of PAT are also able to cause lysis in nonlysogenic strains, presumably by inhibition of peptidoglycan synthesis (authors observations). At 10 µg of PAT per ml an increase in the phage titer[10] and a simultaneous decrease in the Helber chamber cell counts occurred, showing that the lysis could be ascribed to phage development and liberation. At concentrations above 20 µg/ml, however, phage production was inhibited.

25. PAT at 10µg/ml inhibited the replicative DNA synthesis. The inhibition was dose dependent in the concentration range of 10 to 50 µg/ml (Fig. 3). This inhibition was found in toluenized and plasmolyzed cells of *E. coli* D11O (PolA-) and MRE600 (PolA+). In *E. coli* D110 DNA synthesis ceased 30 minutes after addition of PAT, whereas in *E. coli* MRE600 the inhibition was less pronounced and DNA synthesis continued linearly for at least 100 minutes, albeit at a clearly reduced rate (not shown). As the inhibition kinetics resemble those of nalidixic acid, an indirect action on replicative DNA polymerization is suggested.

26. The authors stated that the stimulation of repair synthesis by PAT was dose dependent, the higher dose being more stimulating. They discussed that this may be interpreted as an indication of an increasing number of strand breaks at an increasing concentration of patulin, leading to an increase in repair synthesis. This would mean that PAT causes strand breaks *in vitro* since in the absence of PAT or DNase I only little repair activity is observed, and these breaks are repaired by an intact repair system (Fig. 4).

[10]Phages lyse bacterial lawns on plates to produce plaques, which are used to determine the concentration (titer) of the phages. Phage titer is expressed as the number of plaque-forming units (PFUs) in a given volume.

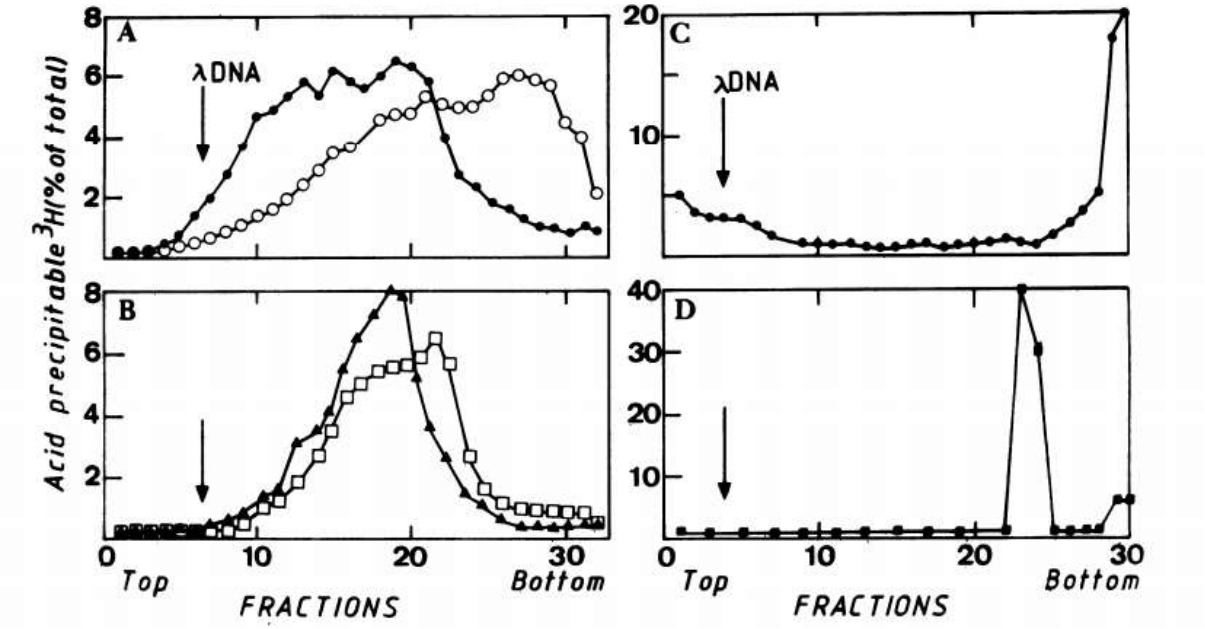

Figure 1. Sedimentation profiles of the DNA from *E. coli* D110 polA in alkaline (A and B) and neutral (C and D) sucrose gradients. (A) Negative and positive control without patulin: ○, control cells; ●, cells irradiated with UV_{254} for 30 s. (B) Cells treated with patulin for 60 min: □, 10 µg/ml; ▲, 20 µg/ml. (C) Cells treated with 25 µg of patulin per ml for 60 min. (D) Cells treated with 50 µg of patulin per ml. (Figure taken from Lee, K.S. and Röschenthaler, 1986).

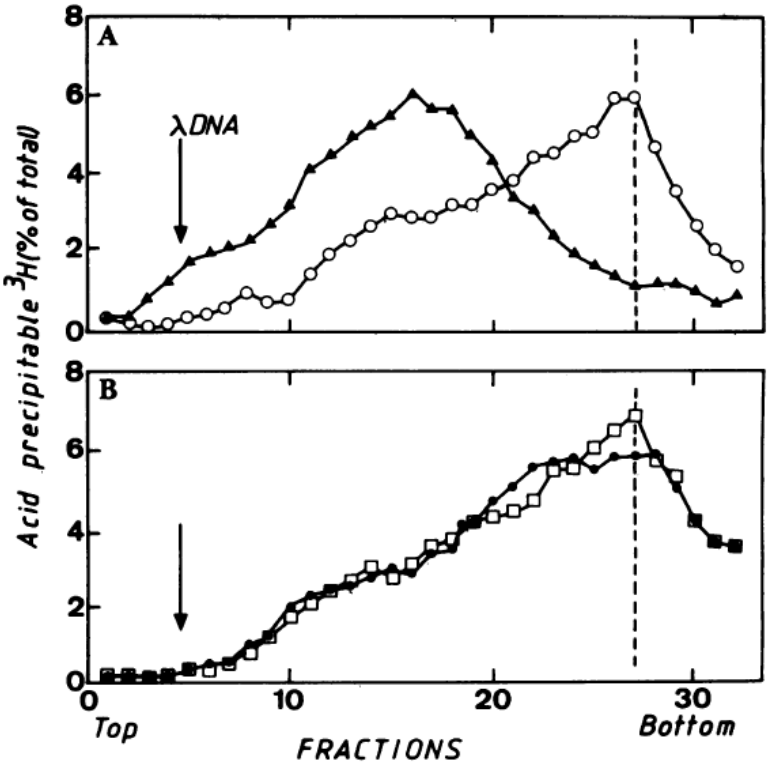

Figure 2. Sedimentation profiles of DNA from E coli MRE600 cells after irradiation with UV_{254} for 60s. Alkaline sucrose gradient analysis. (A) Negative and positive

controls: ○, DNA from untreated control cells; ▲, cells irradiated with UV_{254} for 60 s, no repair incubation. (B) Repair incubation in M-9 salts solution for 90 min ●, without patulin; □, in the presence of 10µg of patulin per ml (Figure taken from Lee, K.S. and Röschenthaler, 1986).

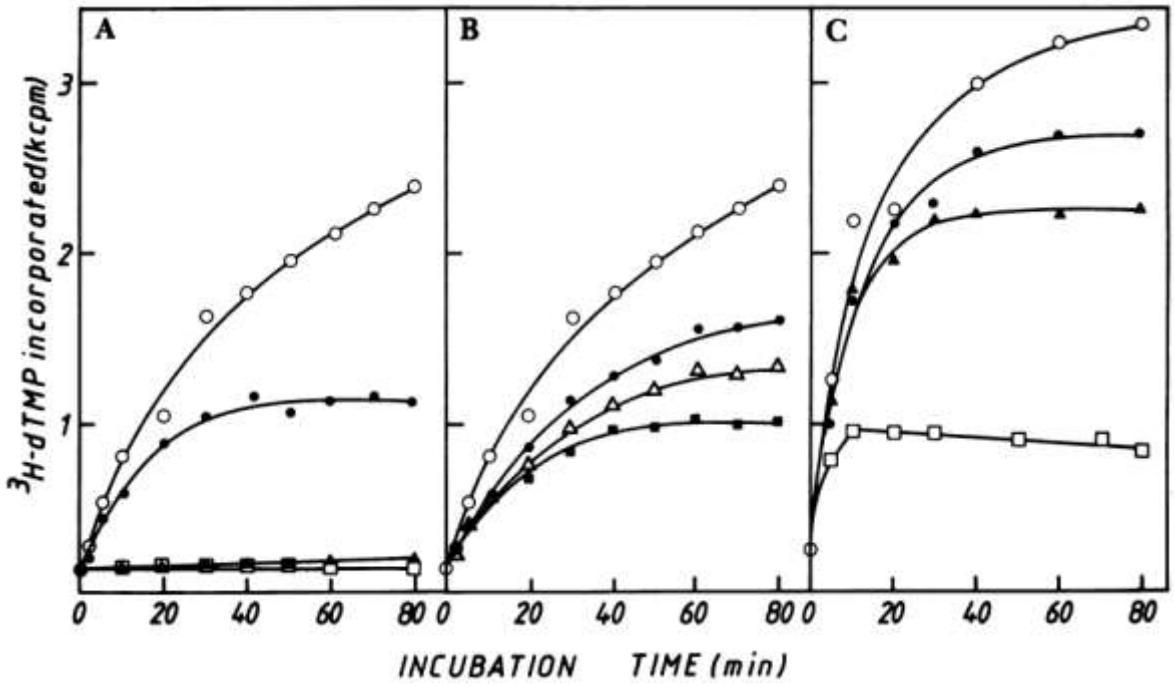

Figure 3. *In vitro* DNA replication synthesis in toluenized (A and B) and plasmolyzed (C) cells of *E. coli* D110 (polA). (A) System control: ○, incorporation of 3H label from [3H] dTTP into acid-precipitable material; ●, incorporation with 200 µg of nalidixic acid per ml present; ▲, without ATP; □, without ATP and NAD. (B) Incorporation in the presence of patulin: ○, control; ●, 10 µg/ml; ∆, 25 µg/ml; ■, 50 µg/ml. (C) Incorporation in the presence of patulin: ○, control, plasmolyzed cells; □, in the presence of 10 µg of DNase I per ml; in the presence of ●, 10 µg, and ▲, 50 µg of patulin per ml. (Figure taken from Lee, K.S. and Röschenthaler, 1986).

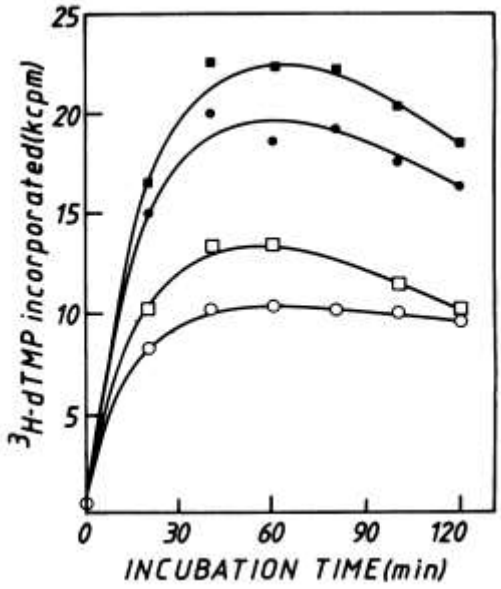

Figure 4. *In vitro* DNA repair synthesis in plasmolyzed cells of *E. coli* MRE600. The synthesis mixtures were incubated with patulin and DNase I at 30°C for 60 min. The synthesis reaction was started by addition of [3H] dTTP at time zero. Symbols: ○, control; □, 0.1 µg of DNase I per ml; ●, 10 µg and ■, 50 µg of patulin per ml. (Figure taken from Lee, K.S. and Röschenthaler, 1986).

Mammalian cells

27. PAT treatment (24 hours) resulted in a concentration-dependent (0, 5, 7, 9 µM) (0, 770.6 , 1078.8, 1387.08 µg/L) reactive oxygen species (ROS) generation accompanied by DNA damage (increase of DNA damage marker H2AX phosphorylation) and p53 activation evidenced by induction of its transcriptional targets Bax and p21 in Human Embryonic Kidney (HEK) 293 cells (Jin *et al*., 2016). HEK293 and mouse embryonic fibroblast (MEF) cells were grown in Dulbecco's Modification of Eagle's Medium (DMEM) supplemented with 10% fetal bovine serum without antibiotics. When cells density reached about 50–60% confluence, the medium was changed with fresh medium containing PAT.

28. Generation of intercellular ROS was measured by flow cytometry following staining with H_2DCFDA, a reduced form of 2,7-dichlorofluorescein. At 30 minutes before harvest, H_2DCFDA was added to the medium to a concentration of 5 µmol/L. The fluorescence was measured using a flow cytometer. The comet assay was carried out after the treatment, the cells were collected and suspended in phosphate-buffered saline (PBS). A mixture of 50 µL cell suspension with 50 µL 1.0% low melting agarose was added onto 0.5% agarose precoated frosted slides. After solidification on ice for 10 minutes, slides were lyzed for 1 hour at 4 °C. Then the slides were put into the electrophoresis solution and the nuclear DNA was allowed to unwind for 20 min. Electrophoresis was conducted subsequently for 20 min at 300 mA, 25 V. After electrophoresis, the slides were neutralized twice for 15 min in neutralization buffer. Before analysis, slides were stained with propidium iodide (PI). Comet images were examined by fluorescence microscope at 200 × magnification.

29. Quantification of DNA damage was analyzed by software programme (CaspLab-Comet Assay Software Project, version 1.2.3b1). The tail moment and the percentage of DNA in the tail (% Tail DNA) were used as DNA damage indicators. Western blotting was carried out by cell lysing with ice-cold RIPA (radioimmunoprecipitation assay) buffer. For testing RNA interference, the cells were transfected with 5 nmol/L of specific or negative control siRNA using INTERFERin siRNA transfection reagent according to the manufacturer's instructions. 24 hours post-transfection, the cells were used for subsequent experiments.

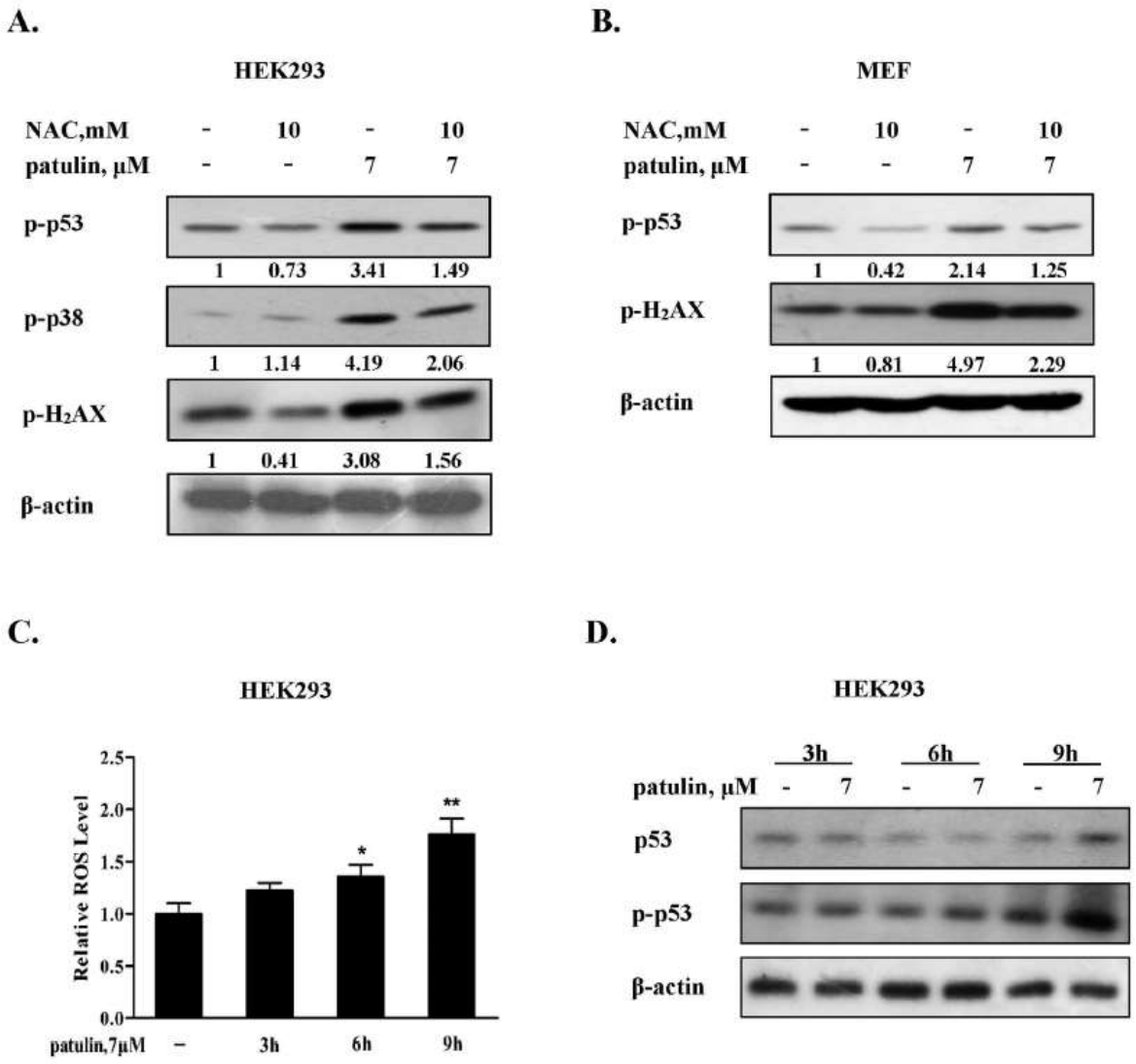

Figure 5. ROS generation preceded p53 activation in response to patulin exposure. (A). Effects of ROS inhibition by NAC on p53, p38 and H2AX phosphorylation by PAT in HEK293 cells. The cells were treated with patulin in the presence or absence of NAC for 24 hours and then the p53 and H2AX phosphorylation were analyzed by western blotting. (B). Effects of ROS inhibition by NAC on p53 and H2AX phosphorylation by patulin in p53 wide type MEF cells. The cells were treated with patulin in the presence or absence of NAC for 12 hours and then p53 and H2AX phosphorylation were analyzed by western blotting. (C). Time-course of ROS

generation by PAT in HEK 293 cells. The cells were treated with PAT for the indicated times and intercellular ROS levels in response to patulin exposure were measured by flow cytometry following staining with H2DCFDA. (D). Time-course analysis of total p53 and p53 phosphorylation. The cells were treated with patulin for the indicated time and then p53 and p53 phosphorylation were assessed by western blotting. n = 3, **P* < 0.05, ***P* < 0.01. (The blots shown are representative of three independent experiments). (Figure taken from Jin *et al*., 2016).

30. As shown in Fig. 5A, PAT treatment resulted in a concentration-dependent ROS generation accompanied by DNA damage (increase of DNA damage marker H2AX phosphorylation) and p53 activation evidenced by induction of its transcriptional targets Bax and p21 (Fig. 5B) in HEK 293 cells. To determine the role of p53 activation in PAT-induced ROS generation, we examined the influences of p53 inactivation by RNAi approach on the levels of ROS. As shown in Fig. 5C, p53 was efficiently inhibited by p53 siRNA. Under such condition PAT induced ROS was significantly decreased compared with that of control siRNA/patulin treatment (Fig. 5D). Consistent with the decreased ROS generation, DNA damage marker H2AX phosphorylation, % tail DNA and tail moment induced by PAT were dramatically ameliorated when p53 was silenced (Fig. 5C, E). Moreover, the functional role of p53 in PAT-induced ROS was further assessed in p53 knockout MEF cells. PAT caused a concentration-dependent increase of both phospho- and total p53 in MEF cells (Fig. 5F). In line with the p53 activation, a significant higher level of ROS was observed in p53 wild type MEF cells than that found in p53 knockout MEF cells (Fig. 5G). Consistent with the levels of ROS, a decreased DNA damage marker H2AX phosphorylation induced by patulin was detected in p53 knockout MEF cells compared with that in p53 wild type MEF cells (Fig. 5F). Taken together, these results clearly indicated that p53 activation functioned as a pro-oxidant mediator to facilitate ROS generation in response to patulin exposure in the cell lines tested. The authors stated that ROS generation preceded p53 activation in response to PAT exposure. To determine the role of ROS generation in PAT-induced DNA damage and p53 activation, they tested effects of ROS inhibition by N-acetyl-1-cysteine (NAC), a precursor of intracellular glutathione synthesis and ROS scavenger, on H2AX, p53 and p38 phosphorylation in response to patulin. As shown Fig. 6A and B, PAT-induced phosphorylation of H2AX, p38 and p53 was obviously attenuated in the presence of NAC in both HEK293 and p53 wt MEF cells. Blockade of ROS led to inhibition of p53 activation, whereas inactivation of p53 resulted in decreased ROS generation in response to PAT exposure (Fig. 5D and G). The authors suggested a feedback loop existing between ROS generation and p53 activation. To determine which one was the primary event, the authors carried out a time kinetic study assessing dynamic changes of ROS generation and p53 phosphorylation. As shown in Fig. 6C and D, exposure to PAT induced a rapid ROS generation and a significant increase of ROS level was detected as early as after 6 hours of PAT exposure, whereas the increased p53 phosphorylation was observed at 9 hours of PAT treatment. These results indicated that p53 activation was initiated by ROS generation and activation of p53 in turn promoted ROS production through regulation of PIG3/catalase axis.

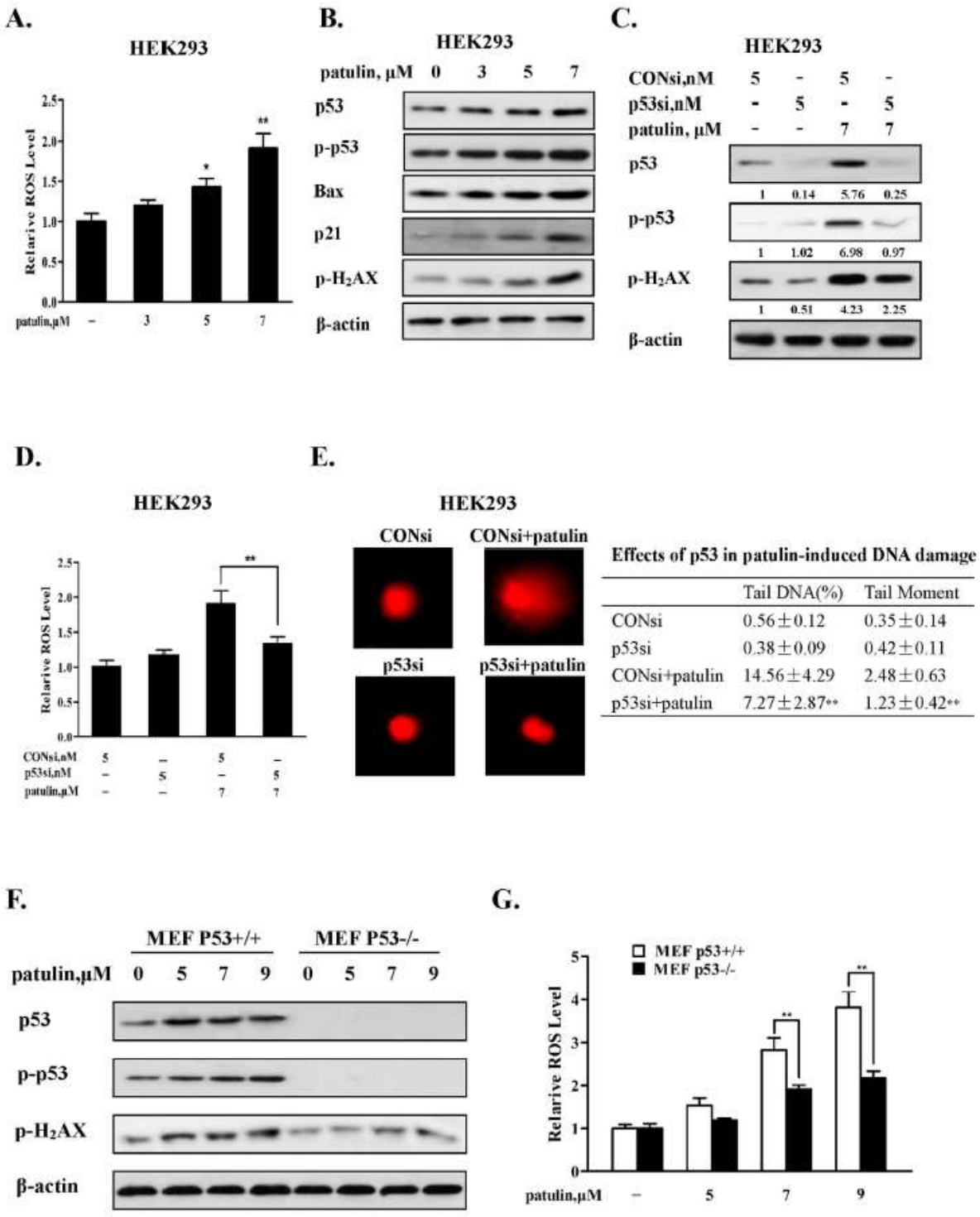

Figure 6. Inactivation of p53 decreased ROS generation in response to patulin exposure. (A). PAT induces ROS generation in a concentration-dependent manner in HEK293 cells. The cells were treated with various concentrations PAT for 24 h and intercellular ROS levels in response to patulin exposure were measured by flow cytometry after staining with H2DCFDA. (B). Effects of PAT on phosphorylation of H2AX and expression of p53, Bax and p21. The cells were treated with various concentrations PAT for 24 h and then the protein levels were analyzed by western blotting. (C). Effects of p53 inactivation by RNA interference on H2AX phosphorylation by PAT. The cells were transfected with p53 siRNA using

INTERFER siRNA transfection agent. At 24 hours post-transfection, the cells were treated with 7 μM PAT for 24 hours and then H2AX phosphorylation was analyzed by western blotting. (D). Effects of p53 knockdown on ROS production by PAT. The cells were transfected with p53 siRNA using INTERFER siRNA transfection agent. At 24 hours post-transfection, the cells were treated with 7 μM patulin for 24 hours and intercellular ROS levels in response to PAT exposure were measured by flow cytometry after staining with H2DCFDA. (E). Effects of p53 inactivation on PAT-induced DNA damage. The cells were transfected with p53 siRNA using INTERFER siRNA transfection agent. At 24 hours post-transfection, the cells were treated with 7 μM patulin for 24 hours and DNA damage in response to patulin exposure were measured by comet assay. Effects of patulin on phosphorylation of H2AX and ROS levels in p53 wild type/knockout MEF cells. The cells were treated with various patulin concentrations for 12 h. H2AX phosphorylation (F) was analysed by western blotting and ROS generation (G) was measured by flow cytometry after staining with H2DCFDA. n = 3, *P < 0.05, **P < 0.01. (The blots shown are representative of three independent experiments). (Figure taken from Jin *et al*., 2016).

31. Alves *et al*., (2000) demonstrated induction of chromosomal aberrations and the formation of micronuclei.

32. PAT (≥98%). Cytokinesis-blocked human lymphocyte micronuclei assay was undertaken using aliquots of 500 μl of whole blood from seven healthy donors which were cultured in 4.5 ml supplemented Ham's F-10. Lymphocytes were stimulated using 25 μl of phytohaemagglutinin (PHA) and incubated at 37°C. After 24 h the cells were exposed to patulin (2.5, 5 and 7.5 μM) (385.3, 770.6 and 1155.9 μg/L) dissolved in DMSO. These doses were chosen from the range of non-cytotoxic concentrations as assessed by the cytokinesis-blocked proliferating index[11] (CBPI). Cytochalasin B was added after 44 hours at a final concentration of 6 μg/ml. After 72 hours culture, cells were harvested by centrifugation, and washed. The cells were again centrifuged, submitted to a mild hypotonic treatment and immediately centrifuged again. The centrifuged cells were placed on dry slides and smears were made. After air drying the slides were fixed for 20 minutes. One day later the slides were stained with Giemsa for 8 minutes.

33. For each experiment, 1000 binucleated lymphocytes with well-preserved cytoplasm were scored. Micronuclei (MN) were identified according to the criteria of Caria *et al*. (1995) using a 500× magnification for detection and a 1250× magnification for confirmation. Control cells included a negative DMSO control, which did not exceed 0.3% (v/v) of the culture medium, and MMC (0.75 μM) as a positive control. Statistical analysis for the comparison of each test dose to the DMSO control was performed using Student's two-tailed t-test. In order to simultaneously compare all the test doses in the dose–response curve, a non-parametric ANOVA (Friedman test) was carried out.

34. The MTT assay (Mitchell, 1988) was performed as follows. Wild-type V79 Chinese hamster cells (approximately 0.5×10^4) were grown for 24 hours in 12-well

[11] This index was calculated according to the following formula:
CBPI = [MI + 2MII + 3(MIII + MIV)]/n as proposed by Surrallés et al. (1995), where MI–MIV represent the number of human lymphocytes with one to four nuclei and n the total number of cells scored.

plates in supplemented Ham's F-10 medium and incubated. PAT (0.35–1.55 µM) was then added and the cells incubated for 20 hours. The medium was removed, the cells washed and then MTT (0.5 mg/ml dissolved in culture medium) was added for a further 4 hours. Cells were treated with DMSO and the absorbance of the converted dye was measured at 570 nm. Cytotoxicity was assessed by comparing the absorbance values of treated cells with control cells. Triplicate assays were performed.

35. A chromosomal aberration assay was done with cultured V79 Chinese hamster cells as described above in supplemented Ham's F-10 medium and incubated. In the first set of experiments to evaluate the genotoxicity of PAT, 24 hour cultures (~5×10^5 cells) growing as monolayers in 25 cm^3 tissue culture flasks were treated with PAT (0.35, 0.5, 0.65, 0.8 and 0.95 µM (53.9, 77.1, 100.2, 123.3, 146.4 µg/L)) dissolved in DMSO. These doses were chosen from the range of non-cytotoxic doses as assessed by the MTT assay, as described above, and by the mitotic index (MI). In the set of experiments to test the anticlastogenic effect of ascorbic acid on the genotoxicity of patulin, three doses of ascorbic acid (0.8, 8.0 and 80.0 µM) were incubated together with a genotoxic dose of PAT (0.80 µM (123.3µg/L)). In all the experiments, the cells were grown for an additional 17 hours and afterwards the medium removed and the cells washed. Colchicine was added at a final concentration of 0.6 µg/ml. Cells were grown for a further 3 hours and then harvested by trypsinisation. After 3 minutes hypotonic treatment was added then the cells fixed and slides prepared and stained with Giemsa for 10 minutes. Three or four independent experiments were carried out for each dose and 100 metaphases were scored. Control cells included a DMSO control, which did not exceed 0.5% (v/v) of the culture medium, and MMC as positive control (0.75 µM). Scoring of the different types of aberrations followed the criteria described by Rueff *et al* (1993). The statistical analysis for comparison of each test dose of PAT to the DMSO control as well as for comparison of ascorbic acid anticlastogenic effects on patulin genotoxicity was performed using Student's two-tailed t-test. In order to simultaneously compare all the test doses in the dose–response curve, a non-parametric ANOVA (Friedman test) was also carried out.

36. Figure 7 shows the average MNBN values (‰) and respective standard deviations from the seven donors studied. The micronucleated cells increased significantly and in a dose–response manner for the three concentrations studied, 2.5, 5.0 and 7.5 µM (385.3, 770.6 and 1155.9 µg/L) ($P < 0.05$, $P < 0.001$ and $P < 0.001$, respectively). The non-parametric ANOVA for simultaneous comparison of all the doses tested revealed a P value <0.001. The highest concentration tested augmented yields of DNA-damaged cells ~3.6-fold when compared with background levels. Table 1 shows that cytotoxicity, as assessed by the mentioned parameters [BN (%) and CBPI], was not present at the concentrations studied. A clear induction of micronuclei in human cells by PAT is shown in both Table 1 and Figure 7. Table 2 presents the raw data from three independent experiments performed with five concentrations of patulin with V79 Chinese hamster cells in the absence of any metabolic activation. Under these experimental conditions, PAT induces not only chromatid and isochromatid aberrations, which are more frequent, but also some chromosomal aberrations in V79 cells. Clastogenic activity was detectable in a very narrow dose range up to concentrations of 1 µM (154.12 µg/L). For higher concentrations PAT is a potent toxic agent for V79 cells (MZ). As shown, for

concentrations >1 µM (154.12 µg/L) there is a considerable decrease in cell viability. Figure 4 presents the average frequencies of CAEG (%) and respective standard deviations from the above- mentioned independent experiments. CAEG increased in a dose-dependent manner up to 0.8 µM (123.3 µg/L) (~10-fold the background genotoxicity to DMSO control cells). The genotoxicities of the doses 0.65, 0.8 and 0.95 µM (100.2, 123.3, 146.4 µg/L) were significantly different from that observed in DMSO control cells ($P < 0.05$, $P < 0.05$ and $P < 0.01$, respectively). Non-parametric ANOVA for simultaneous comparison of all the doses tested revealed a P value <0.05. The authors stated that Figure 8 and Table 2 unequivocally show genotoxicity of PAT in V79 cells.

Table 1- Induction of micronuclei in cytokines-blocked human lymphocytes from seven healthy donors by PAT. Table taken from Alves *et al* (2000)

Donor	Patulin (μM)	BN (%)	PolyN (%)	Met (%)	CBPI	MNBN (‰)
1	DMSO	40.8	17.1	3.5	1.71	0
	2.5	45.9	5.9	0.8	1.55	8
	5.0	34.8	1.9	0.9	1.38	9
	7.5	47.1	8.3	1.9	1.62	19
	MMC[a]					
2	DMSO	44.8	3.9	1.0	1.46	8
	2.5	51.1	10.9	1.1	1.72	14
	5.0	42.3	5.5	1.5	1.51	20
	7.5	48.5	7.2	0.9	1.63	20
	MMC	43.9	1.3	1.0	1.45	74
3	DMSO	49.1	4.8	1.7	1.59	5
	2.5	46.4	5.3	1.7	1.58	5
	5.0	42.0	3.0	1.6	1.49	10
	7.5	42.7	2.3	1.6	1.47	19
	MMC	48.8	2.1	1.0	1.53	50
4	DMSO	46.3	6.7	2.8	1.61	4
	2.5	45.5	6.2	2.4	1.62	10
	5.0	46.0	4.6	2.1	1.56	16
	7.5	43.2	9.1	2.6	1.63	17
	MMC	43.2	2.6	2.3	1.51	52
5	DMSO	50.9	4.9	1.0	1.61	10
	2.5	52.1	10.4	1.3	1.74	14
	5.0	55.0	4.4	1.5	1.65	20
	7.5	55.5	5.4	1.2	1.67	26
	MMC	51.2	4.5	0.9	1.61	52
6	DMSO	42.1	12.3	2.4	1.68	4
	2.5	45.4	11.4	1.5	1.69	10
	5.0	43.1	14.3	2.1	1.73	16
	7.5	41.1	6.8	1.2	1.55	17
	MMC	46.1	14.0	3.8	1.77	44
7	DMSO	54.6	7.0	1.8	1.70	8
	2.5	44.6	4.7	3.2	1.60	16
	5.0	48.5	3.7	1.9	1.57	16
	7.5	56.1	6.3	2.2	1.70	24
	MMC	51.3	4.2	2.1	1.61	20

MMC, mitomycin C, positive control (0.75 μM); DMSO, dimethylsulphoxide, negative control; BN, binucleated lymphocytes; PolyN, lymphocytes with three or more nuclei; Met, metaphases; CBPI, cytokinesis-blocked proliferating index; MNBN, micronucleated cytokinesis-blocked lymphocytes (binucleated).
[a]Cytotoxic dose of the positive control (1.5 μM MMC).

Table 2: Chromosomal aberrations by PAT in V96 Chinese hamster cells (MZ). Table taken from Alves *et al*. (2000)

Exp.	Conc. (μM)	Ctg	Ctb	Int	Chg	Chb	Isob	Dic	Oth	>10	CAIG (%)	CAEG (%)	MI (%)
1	DMSO	4	2	0	0	0	0	0	0	0	6	2	5.1
2		2	1	0	0	0	0	0	0	0	3	1	3.7
3		2	1	0	0	0	0	0	0	0	3	1	3.9
1	0.35	9	3	0	0	6	1	2	0	0	12	7	
2		8	1	0	1	0	0	0	0	0	11	2	
3		1	0	0	1	2	0	0	0	0	4	2	
1	0.50	14	3	0	0	6	3	0	0	0	16	9	
2		2	1	0	0	0	1	1	0	0	5	3	
3		1	0	0	1	2	0	0	0	0	4	2	
1	0.65	8	3	0	0	2	2	0	1	0	12	6	
2		14	5	0	2	1	1	0	2	0	22	10	
3		1	4	0	1	4	1	1	1	0	13	11	
1	0.80	7	9	0	0	0	4	3	1	0	21	16	
2		8	1	0	0	3	5	1	0	0	17	9	
3		5	2	0	0	4	7	2	1	1	22	17	
1	0.95	3	6	1	0	0	2	0	1	0	13	10	3.6
2		7	3	1	0	3	1	0	0	0	14	7	2.8
3		6	3	0	1	3	1	2	0	0	16	9	2.2
1	MMC	8	8	2	2	3	4	0	6	0	28	21	
2		3	9	3	0	2	0	0	0	0	18	13	
3		3	4	0	1	2	2	0	0	0	12	8	

Results are from three independent experiments for each tested dose.
DMSO, dimethylsulphoxide, negative control; Ctg, chromatid gap; Ctb, chromatid break; Int, interchanges; Chg, chromosome gap; Chb, chromosome break; Isob, isobreak; Dic, dicentric chromosomes; Oth, other aberrations; >10, multi-aberrant cells; CAIG, chromosomal aberrant cells including gaps; CAEG, chromosomal aberrant cells excluding gaps; MI, mitotic index; MMC, mitomycin C, positive control (0.75 μM).

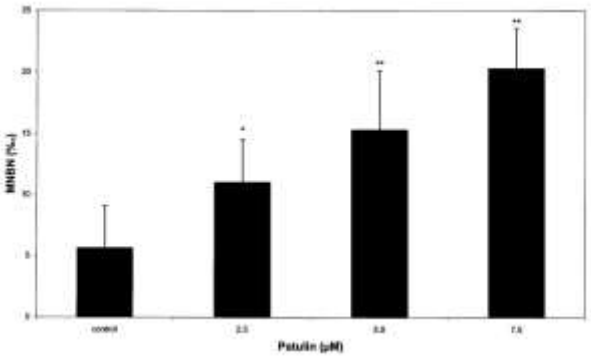

Figure 7. Induction of micronuclei in cytokinesis-blocked human lymphocytes (MNBN) by patulin. Results are the average MNBN values and respective standard deviations from seven healthy donors. *P < 0.05, **P < 0.001, Student's t-test, when compared with DMSO control cells. Non-parametric ANOVA for simultaneous comparison of all doses tested revealed a P < 0.001. Figure taken from Alves *et al*. (2000)

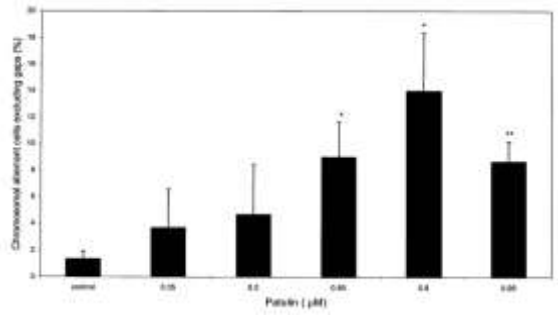

Figure 8. Induction of chromosomal aberrations by patulin in V79 Chinese hamster cells. Results are the averages and standard deviations of three independent experiments. *P < 0.05, ** P < 0.01, Student's t-test, when compared with DMSO control cells. Non-parametric ANOVA for the simultaneous comparison of all doses tested revealed a P < 0.05. Figure taken from Alves *et al*. (2000)

37. Another study by Donmez *et al* (2013) also evaluated the genotoxic potential of PAT using the cytokinesis-block micronucleus cytome (CBMN Cyt) assay with human peripheral blood lymphocytes nucleoplasmic bridges.

38. Approximately 10 ml of peripheral blood samples were collected from 10 healthy non-smoking individuals, of both genders, aged 20–35 years, with no history of exposure to any genotoxic agent. The local ethics committee approved the study protocol (No. 2008/248). The study was conducted in accordance with the Helsinki Declaration and local laws. Each blood donor completed a questionnaire, designed to obtain their exposure history and current health status; and informed consent forms were signed by each of them. The study excluded volunteers who reported alcohol, tea or/and coffee consumption, treatment for acute infections and/or chronic non-infectious diseases different dietary habits, intake of vitamin preparations, or intensive sport activities a week before the beginning of the study. No subject reported medicinal treatment over the 6 months before blood sampling, had a history of occupational and environmental exposure to known genotoxic chemicals/radiation,

or had specific diseases such as hypertension, diabetes mellitus, hypercholesterolaemia, heart diseases or cancer.

39. Heparinized blood samples (~0.4 ml) were incubated for 72 h at 37 °C in 5 ml of peripheral blood karyotyping medium supplemented with 2 % PHA. Two parallel cultures of each person were made for each concentration of PAT. At 24 hours, PAT was added to the cultures. The cultures were treated for 48 hours with PAT at seven concentrations (0.1, 0.3, 0.5, 1, 2.5, 5, and 7.5 µM-15.4, 46.2, 77.1, 154.1, 770.6 and 1155.9 µg/L). In all experiments, doses were chosen from the range of non-cytotoxic concentrations as assessed by the percentages of BN cells and the NDI values. Additional cultures were incubated with MMC as a positive control and DMSO as a vehicle control; these cultures contained 0.84 % of the MMC and 0.4 % DMSO. CBMN Cyt assay was performed as described by Fenech (2000, 2006, 2007) with some modifications. After 44 hours of incubation, cyt-B at the final concentration of 3 µg/ml was added to cultures to block cytokinesis. The cultures were stopped at 72 hours, treated with hypotonic solution (0.1 M KCl) for 4 minutes and fixed (Donmez-Altuntas *et al*. 2003, 2007; Hamurcu *et al*. 2011). The fixed cells were spread onto clean glass slides and stained with 5 % Giemsa for 10 minutes. All slides were coded and read blind. A score was obtained for slides from each duplicate culture from two different scorers using identical microscopes For each concentration and control, every subject was analyzed for the total number of MNi, NBPs and NBUDs per 1,000 BN cells to determine DNA damage effects, when 1,000 BN cells with two macronuclei surrounded by cytoplasm and a cell membrane obtained from whole-blood cultures were scored. The frequency of BN cells containing one or more MN was also determined. In addition, the cells in metaphase were scored when BN cells were scored. The number of necrotic and apoptotic cells were scored in 1,000 mononucleated cells to determine cytotoxicity and the criterion for the identification of necrotic and apoptotic cells was according to Fenech (2007). The number of mono-, bi- and multinucleated cells per 1,000 viable mononucleated cells to determine cytostatic effects was scored in peripheral blood lymphocytes of all individuals. The nuclear division index (NDI) has been calculated by using the formula NDI ¼ ð Þ M1 þ 2 M2 þ 3 M3 þ 4 M4 =N; where M1–M4 represent the number of cells with 1–4 nuclei and N is the total number of viable cells scored (excluding necrotic and apoptotic cells) (Eastmond and Tucker 1989; Fenech 2007)

40. Statistical comparisons on CBMN Cyt assay parameters between treated and control groups were made using Friedman and Wilcoxon nonparametric tests for K-related samples and two-related samples, respectively. Differences between treated and control groups were considered significant at $p < 0.05$ and $p<0.01$. The relationship of CBMN Cyt assay parameters with concentrations of PAT was evaluated by Spearman's rho correlation analysis. Significant levels were set at $p<0.05$ and $p<0.01$. All analyses were conducted using the SPSS for Windows statistical package, version 11.0. The effects of PAT on DNA damage parameters including the number of BN cells with MN, total number of MN in BN cells, distribution of BN cells with MN, MN frequency (%) in BN cells and number of BN cells with NPBs and NBUDs in the human lymphocytes are summarized in Table 3. Not all DNA damage parameters in the vehicle (DMSO) control group were significantly different from the negative control group ($p>0.05$). The number of BN cells with NPBs was significantly increased at PAT concentrations of 5 and 7.5 µM

(385.3 and 1155.9 µg/L) in comparison with the negative control group ($p<0.05$). Also, at the different PAT concentrations, except for NPBs, all other DNA damage parameters were not significantly different from the DMSO control group ($p>0.05$). The positive control (MMC 0.5 µM) was shown to significantly induce all the DNA damage parameters, except the number of BN cells with 2 MN, in comparison with the negative control group ($p<0.05$ and $p<0.01$).

41. With respect to DNA damage effects of PAT on human lymphocytes, PAT induced a statistically significant concentration-dependent increase in the number of BN cells with NPBs in human lymphocytes. PAT was found to induce nucleoplasmic bridges (NPBs) at 5.0 and 7.5 µM (385.3 and 1155.9 µg/L) concentrations ($P<0.05$). In more detail, PAT induced a statistically significant concentration-dependent increase in the number of binucleated cells with NPBs in human lymphocytes, at least at between 7.5 and 5 µM (r 0.771; $p<0.01$), 7.5 and 2.5 µM (r 0.810; $p<0.01$), 5 and 2.5 µM (r 0.883; $p<0.05$), 2.5 and 1 µM (r 0.765; $p<0.05$), 1 and 0.1 µM (r 0.900; $p<0.01$), 0.5 and 0.1 µM (r 0.713; $p<0.05$), and 0.3 and 0.1 µM (r 0.789; $p<0.01$) concentrations tested.

Table 3 The results of DNA damage in PAT concentrations, negative control, vehicle (DMSO) control and positive control (MMC; 0.5 µM) in peripheral blood lymphocytes of 10 healthy individuals (mean ± SD). Table taken from Donmez *et al* (2013).

Group	No. of BN cells with MN	Total no. of MN in BN cells[a]	Distribution of BN cells with		MN Frequency in BN cells (%)	No. of BN cells with NPBs	No. of BN cells with NBUDs
			1MN	2MN			
Negative control	3.60±2.22	3.80±2.39	3.40±2.12	0.20±0.42	0.38±0.24	5.50±5.21	4.10±3.90
Vehicle control	3.90±3.73	4.00±3.83	3.80±3.65	0.10±0.32	0.40±0.38	8.60±6.15	6.60±7.65
0.1 µM PAT	4.10±3.11	4.40±3.60	3.80±2.70	0.30±0.67	0.44±0.36	7.60±6.43	4.80±3.88
0.3 µM PAT	4.20±3.80	4.50±4.14	3.80±3.39	0.40±0.70	0.46±0.43	7.00±6.07	4.00±4.90
0.5 µM PAT	3.50±4.20	3.60±4.48	3.40±3.92	0.10±0.32	0.32±0.45	7.70±9.60	4.30±7.17
1 µM PAT	2.80±3.12	2.90±3.41	2.70±2.83	0.10±0.32	0.29±0.34	7.10±7.59	6.20±8.82
2.5 µM PAT	3.40±3.20	4.00±3.65	2.90±3.00	0.40±0.97	0.40±0.37	11.20±12.27	6.20±5.92
5 µM PAT	3.50±2.68	3.70±3.02	3.20±2.25	0.30±0.68	0.37±0.33	16.70±20.28*,#	5.70±6.60
7.5 µM PAT	5.60±5.27	6.10±6.19	5.10±4.43	0.50±1.08	0.61±0.62	13.40±12.13*,#	5.90±6.86
Positive control	17.40±12.91*,#	18.60±13.35*,#	16.90±12.32*,#	0.60±0.70	1.68±1.48*,#	13.50±15.75*,#	11.20±7.94*,#
Friedman *p*	0.002	0.001	0.002	0.289	0.012	0.036	0.014
Wilcoxon *p*[b]	0.007*	0.007*	0.007*	>0.05	0.017*	<0.05*	0.008*
Wilcoxon *p*[c]	0.007#	0.007#	0.007#	>0.05	0.014#	<0.05#	0.032#

MN Micronucleus, *BN cells* binucleated cells, *NPBs* nucleoplasmic bridges, *NBUDs* nuclear buds; *SD* standard deviation

[a] Total number of MN : (1MNX1)+(2MNX2)

[b] Statistically significant when compared to the negative control.*<0.05 and <0.01

[c] Statistically significant when compared to the vehicle control.#<0.05 and <0.01

42. A study by Zhou *et al*., 2010 demonstrated that DNA damage was induced by PAT as measured by single cell gel electrophoresis (SCGE) assay in HepG2 cells exposed to PAT (0, 5, 10, 20 and 40 mM- 0, 0.77, 1.5, 3.1 and 6.2 µg/ml) for 1 hour. Significant DNA strand breaks were detected after treatment with PAT (20, 40 mM- 3.1 and 6.2 µg/ml) in HepG2cells ($P<0.01$).

43. The SCGE assay was performed as described by Singh and Stephens with slight modifications (Singh and Stephens, 1997). Cells were exposed to PAT (98%) (0, 5, 10, 20, 40 mM- 0, 0.77, 1.5, 3.1, 6.2 µg/ml) for 1 hour at 37°C. Hoechst 33342 (8 mg/ml) and trypan blue (50 mg/ml) were employed to detect the apoptotic cells

and cell viability, respectively. Only cell suspensions with viabilities larger than 90% and no apoptotic cells were used to determine DNA migration on gels. Cell suspension was mixed with 1% LMP agarose and added to fully frosted slides that had been covered with a layer of 1.5% NMP agarose. The cells were then lysed for 1 hour at 4 °C. After lysis, the slides were placed on an electrophoresis unit filled with fresh electrophoretic buffer and left for 20 minutes for DNA unwinding and then electrophoresed for 30 minutes at 18 V and 200 mA. Afterwards, the slides were neutralized with 0.4 M Tris buffer (pH 7.5) and stained with 50 ml of ethidium bromide (20 mg/ml). Finally, the slides were viewed using an Olympus BX-51 fluorescent microscope (excitation filter 549 nm, barrier filter 590 nm). Images of 50 randomly selected cells from each slide were analyzed with Comet Assay Software Project casp-1.2.2 (University of Wroclaw, Poland). Three independent experiments were carried out in every case. The following parameters were evaluated: tail length (mm), tail DNA (%) and tail moment.

44. To investigate the role of GSH in PAT-induced DNA damage, HepG2 cells were pre-cultured with BSO (150 mM) in MEM for 20 hours to deplete the intracellular content of GSH by inhibiting its synthesis, and then exposed to PAT (0, 5, 10, 20, 40 mM-0, 0.77, 1.5, 3.1, 6.2 µg/ml) for another 1 hour.

45. The effect of PAT on the p53 protein level was examined, the authors reasoning was that p53 is a well-known DNA damage marker. For western blotting analysis, aliquots of the cell lysates, were prepared in a lysis buffer. Cell debris and particulate fractions were removed by centrifugation at 13,000 µg for 20 minutes, at 4°C. Protein concentration was measured. The proteins were diluted with 2x sample buffer containing b-mercaptoethanol and bromophenol blue and then heated at 100 °C for 5 min. Proteins were separated by 10% SDS-PAGE, transferred onto PVDF membranes, and subjected to immunoblot analysis using the respective antibody against: phosphor-p53, p53 and b-actin. Immunoreactive Proteins were subsequently detected with appropriate secondary antibodies conjugated with peroxidase-conjugated AffiniPure. Band density was determined using synGene Gene Tools software. The relative densities phosphor-p53 and p53 to b-actin were calculated.

46. Table 4 shows the numerical values for tail length, tail DNA (%) and tail moment in HepG2 cells that were exposed to PAT (0, 5, 10, 20, 40 mM-0, 0.77, 1.5, 3.1 and 6.2 µg/ml) for 1 hour. In all groups, the cell viabilities were consistently larger than 90% and no apoptosis was observed (data not shown). Significant DNA strand breaks were detected after treatment with PAT (20, 40 mM- 3.1 and 6.2 µg/ml) in HepG2 cells ($P < 0.01$). When HepG2 cells were treated with PAT (0, 0.19, 0.38 and 0.75 mM-0.03, 0.06 and 0.12 µg/ml) for 24 hours significant increase of p53 protein was observed at the concentrations of 0.38 and 0.75 mM (0.06 and 0.12 µg/ml) ($P < 0.05$ or $P < 0.01$) (Figure 9). The authors noted that the phospho-p53 (serine 15) protein was not detected.

Table 4 DNA strand breaks induced by PAT in HepG2 cells measured by SCGE assay. (Table taken from Zhou *et al*., 2010).

PAT (μM)	Tail length (μm)	Tail DNA (%)	Tail moment (μm)
0	3.25±0.07	3.26±0.28	0.15±0.05
5	3.56±0.20	4.59±0.37	0.19±0.03
10	4.63±0.10	4.58±0.51	0.30±0.01
20	35.40±2.47**	25.94±1.09**	12.57±1.33**
40	46.60±2.39**	47.53±1.12**	24.95±1.55**

DNA damage as measured by SCGE assay in HepG2 cells exposed to PAT (0–40 μM) for 1 h. Data represented the mean value ± S.D. obtained with three independent experiments per exposure concentration. **$P < 0.01$ significantly different from cells without PAT.

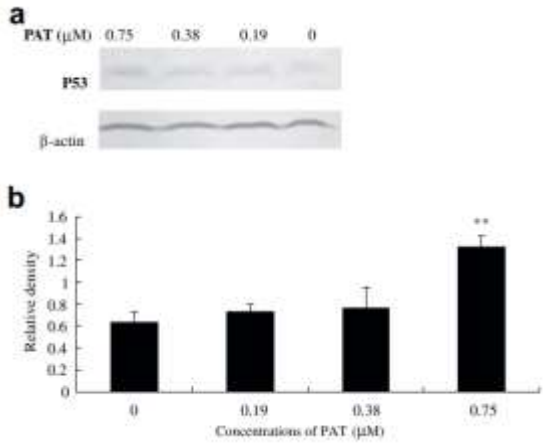

Figure 9. Expression of p53 protein in HepG2 cells treated with PAT (0–0.75 mM) for 24 h. Western blot analysis (a) and densitometry (b). **P < 0.01 significantly different from cells without PAT. (Figure taken from Zhou *et al*., 2010).

47. Another study using the SCGE assay with HEK293 cells treated with PAT (5, 10, 15, 20 µM- 770.6, 1541.2, 6935.4 and 3082.4 µg/L) for 2 hours demonstrated DNA damage on a single cell basis (Liu *et al*., 2003).

48. Sister chromatid exchange was carried out as follows: The CHO-K1 cells (1 x 10^5 cells) were grown for 18 hours, and then various concentrations of mycotoxin and 5-bromo-2-deoxyuridine (BrdU) (8 µg/ ml) were added. The cultures were incubated in the dark for a further 42 hours and metaphase was blocked during the last 2 h with 0.1 µg/ml colcemid. For treatment of human peripheral blood lymphocytes, toxins and BrdU (10 µg/ml) were added to cultures for 40 hours and Colcemid (0.1 µg/ml) was added 25 minutes prior to harvest. At the end of the culture period cells were harvested, exposed to a hypotonic solution and fixed. Chromosome spreads were obtained using the standard air drying techniques. Visualization of SCEs was accomplished by a modification of the fluorescence plus Giemsa techniques (Becher and Sandberg, 1982). Briefly, slides mounted with Hoechst 33258 were put on the slide warmer at 56°C and exposed to UV light for 30 min. Slides were well-rinsed with distilled water, dried, and subsequently stained with Giemsa stain. A total of 75 second-division metaphases from three independent cultures were scored (number of SCE/cell) for each experimental point.

49. The CHO-K1 cells and human lymphocytes were cultured as described in the SCE assay. The cultures were incubated with various concentrations of PAT for 42 h and metaphase was blocked with 0.1 µg/ml Colcemid. Cells were harvested, treated with hypotonic solution, and fixed. Slides were prepared and stained with Giemsa. Two independent experiments were carried out for each concentration and 100

metaphases were scored in each experiment. To evaluate the clastogenic activity of mycotoxins, the total number of DNA gaps and breaks, including both chromosome-type and chromatid-type gaps and breaks, were scored according to the criteria described by Dean and Danford (1984). The average number of DNA gaps and breaks in 100 metaphases from two separate experiments is expressed as mean ± SE.

50. SCGE assays were primarily conducted using a protocol reported by Wang *et al*. (2001) according to the guidelines developed by Tice *et al*. (2000). Briefly, HEK293 (1 x 10^5 cells) were cultured in medium containing vehicle alone or various concentrations of PAT for 2 hours. These concentrations of PAT were chosen from the range of noncytotoxic concentrations as assessed by the MTT assay. The adherent cells were then trypsinized and mixed with 1% low-melting-point agarose at 42°C. The mixtures were immediately transferred to the CometSlide and the slides were immersed in ice-cold lysis solution for 1 hour. After electrophoresis in an alkaline buffer at 300 mA for 30 min, DNA on the slides was stained with SYBR green I. To conduct formamidopyrimidine-DNA glycosylase (Fpg) enzyme-modified assay, slides after lysis treatment as described above were incubated with enzyme reaction buffer at 37°C for 1 hour. Then 5 units of bacterial Fpg in 20 µl of reaction buffer were applied to each sample on slides. After incubation at 37°C for another 1.5 hours, slides were subjected to electrophoresis and staining as previously described. The image of each cell on slides was visualized and photographed under a fluorescence microscope. Image analysis was performed with the computer software from Euclid Analysis. Parameters derived from the image included tail moment and percentage DNA. For each experimental point, three cultures were treated with toxins independently, and the DNA damage level of 50 cells was measured from each culture.

51. CHO-K1 cultures treated with 0.3 µM (46.2 µg/L) of PAT showed significant levels of DNA gaps and breaks (50 ± 2 per 100 metaphases) in comparison with control (31 ± 3 per 100 metaphases), suggesting the potential clastogenicity of PAT. The authors reported that no elevated level of DNA gaps and breaks was observed in lymphocytes incubated with 0.1 to 0.3 µM (15.4- 46.2 µg/L) of PAT. The effects of PAT on DNA damage in HEK293 cultures are shown in Table 4. Exposure of the cells to concentrations of 15 µM (2311.8 µg/L) or greater caused a significant and concentration related increase in the tail moment and percentage DNA values. The tail moments of cells after exposure to 20 µM (3082.4 µg/L) PAT were 2.75 fold higher than those in control, which the authors suggested this indicated that PAT treatment generated direct strand breaks and/or alkali labile sites in HEK293. Hydrogen peroxide (H_2O_2), a potent inducer of oxidative DNA damage, was used as a positive control in the assay (Liu *et al*., 2003).

Table 5. The effects of PAT on DNA migration in the SCGE assay with HEK293. (Table taken from Liu *et al*., 2003).

The effects of PAT on DNA migration in the SCGE assay with HEK293

Treatment	Tail moment	Percent DNA
Patulin (μM)[a]		
1	2.00 ± 0.39	8.13 ± 0.94
5	2.00 ± 1.00	11.00 ± 1.10
10	2.66 ± 0.77	15.08 ± 3.80
15	4.89 ± 1.18*	15.51 ± 1.56*
20	5.50 ± 1.07*	19.72 ± 1.47*
H_2O_2(μM)[b]		
0	1.65 ± 0.35	8.93 ± 2.75
10	2.77 ± 0.27	21.88 ± 0.88*
40	7.92 ± 0.42*	32.10 ± 2.40*

[a] Cells exposed to various concentrations of PAT for 2 h.
[b] Cells exposed to various concentrations of H_2O_2 for 30 min.
* Significantly different as compared to the control values ($p < 0.05$).
Data are mean ± SE derived from three separate experiments.

52. In the micronucleus (MN) assay PAT concentrations (0.1 and 0.5 µM-15.4 and 77.06 µM) for 6 hours to V79 cells revealed that PAT induced MN in a concentration-dependent manner (Pfeiffer *et al.*, 1998). Micronucleus assay and CREST staining were carried out by V79 cells being spread on slides and exposed to PAT concentrations for 6 hours. The slides were then briefly immersed in PBSCMF and subsequently kept in fresh DMEM for various lengths of time. After washing in PBS-CMF, fixation in 2% aqueous paraformaldehyde solution for 5 minutes and further washing, slides were kept in methanol at –20°C for at least 1 hour, subsequently immersed in acetone at –20°C for 10 minutes and then washed with PBS-CMF three times for 5 minutes each. To block non-specific binding sites, 100 µl goat serum (Life Technologies, Eggenstein, Germany) was spread on each slide using a coverslip. After 1 hour at 37°C in a water saturated chamber, the coverslips were removed and the slides immersed in PBS-CMF. The same incubation and washing procedure was subsequently repeated with 100 µl of a solution of CREST antibody and subsequently with fluorescein isothiocyanate-conjugated goat anti-human IgG1 (Sigma; diluted 1:200 with PBS-CMF containing 1% BSA). Slides were then kept for 12 hours in Soerensen buffer, pH 8.0, prior to staining with antifade solution (30 µl/slide) containing DAPI (2.5 mg/ml) and propidium iodide (1 mg/ml). Samples of 3000 cells/slide were then examined for MN and CREST signals by fluorescence microscopy. Micronuclei were determined according to the criteria established by Countryman and Heddle (1976).

53. Furthermore, in order to analyse PAT for clastogenic potential, the time course of MN formation was studied. V79 cells were treated for 6 hours with 0.5 µM (77.06 µg/L) PAT, followed by incubation with fresh medium for various lengths of time up to 24 hours (3, 6, 12 and 24 hours). The number of CREST-positive MN (micronuclei containing whole chromosomes/chromatid) showed a peak at 6 hours post-treatment with a fairly constant level of ~35 MN before and after this time point. In contrast, no CREST-negative MN (micronuclei containing acentric chromosomal fragments) were observed at 3 or 6 hours, but their number increased steeply between 12 and 24 hours. The authors stated that the aneuploidogenic and clastogenic potential of PAT may well contribute to the putative carcinogenicity. This formation of micronuclei is seen in other studies such as Glaser and Stopper (2012). Micronucleus (MN) and nucleoplasmic bridge (NPB) analysis was carried out by cells (2 X 10^5) being seeded the day before in 3 mL well plates and were incubated for 20 hours with 20 µM BSO. Subsequently, cells were washed and treated with 0.5 µM (77.06 µg/L) PAT. After 4 hours PAT was removed and the cytokinesis inhibitor cytochalasin B (5 µg/ mL) was added, yielding a high number of binucleated cells after a 20 hour post-incubation time. By limiting the analysis to such

binucleated cells, it was ensured that the cells have actively divided since the treatment. For the time course of MN and NPB formation, cells seeded the day before, were incubated for the indicated time with 0.5 µM (77.06 µg/L) PAT and 5 µg/mL cytochalasin B simultaneously. Cells were brought onto glass slides by cytospin centrifugation and fixed in methanol (20 °C, ≥1 hour). Slides were stained with Gel Green (Biochrom, 1:1000 in PBS for 3 min). From each of two slides, 1000 binucleated cells were evaluated with regard to frequencies of micronucleus-containing and NPB-containing cells. Cytokinesis block proliferation index (CBPI) was calculated in 1000 cells per slide using the formula:

CBPI = [MI + 2MII + 3 (MIII + MIV)] with MI–MIV representing the number of cells with one to four nuclei (Surralles *et al*., 1995).

54. MN and NPB were scored according to the criteria defined by the members of HUman MicroNucleus (HUMN) project (Fenech *et al*., 2003). Structures were defined as MN if they were round or oval, had the same staining intensity as the main nuclei and were not connected to them. Continuous links between the nuclei in binucleated cells were scored as NPBs. The damaged cell was considered as endpoint, therefore cells containing more than one MN or NPB were scored as one cell with one or more micronuclei or bridge, respectively. For kinetochore analysis cells were treated for 4 hours with 0.5 µM (77.06 µg/L) PAT followed by 20 hour post-incubation with cytochalasin B (5 µg/mL). Cells were brought onto glass slides by cytospin centrifugation and fixed in methanol (20°C, ≥1 hour). Kinetochores were stained with a first antibody against centrosomes (Positive Control Serum (Centromere), undiluted, 37°C, overnight) and a rhodamine conjugated secondary antibody (1:20, 37 °C, 2 hours). Counter staining of nuclei was done with chromomycin A (50 µM, 3 min). About 5600 cells were evaluated for the presence of kinetochore-positive or -negative MN.

55. For the detection of cross-links a modified protocol has be proposed by Olive *et al*. (1990). By creating DNA cross-links DNA fragments resulting from treatment with radiation or strand breaking agents are artificially increased in size and their migration in an electrical field is impeded. V79 cells (5 x 10^5), seeded the day before, were treated for 4 hours with 0.5 µM (77.06 µg/L) PAT. After a washing step 100 µM H_2O_2 was added for 30 minutes. Subsequently, the cells were harvested and used in the comet assay described above (Schupp *et al*., 2011) using a fluorescence microscope at 200-x magnification and computer aided image analysis (Komet 5). Twenty five cells from each of two slides stained with Gel Red (Biochrom, 20 µg/mL in PBS) were measured, with percent tail DNA as the evaluation parameter. Overall, the study demonstrated induction of micronuclei (MN) and nucleoplasmic bridges (NPB) in 1000 binucleated (BN) cells were observed in V79 cells treated with 0.5 77.06 µg/L) PAT for 3, 4.5 and 6 hours. By using a modified version of the alkaline comet assay it demonstrated DNA damage induced by H_2O_2 with or without pretreatment with the known cross-linking agent cis-platin or PAT.

56. Schumacher *et al* (2006) assessed the potential of PAT to induce DNA strand breaks and oxidative DNA base modifications by suspending V79 cells treated with PAT for 1 hour (0, 0.5, 1, 5, 10, 50 and 100 µM-0, 77.06, 154.12, 770.6, 1541.2 and 7706 µg/L) and 4 hours (0, 0.4, 0.8, 1.2, 1.6, 2, 2.4 µM-0, 61.6, 123.3, 184.9, 246.6, 308.2, 369.9 µg/L). Induction of DNA–DNA interstrand cross-links was also tested in

V79 cells at a concentration of 1.5 µM (231.18 µg/L) (PAT for 6, 12, 18 and 24 hours; in a side experiment cells were also treated with 0.4, 0.8, 1.2 and 1.6 µM (61.6, 123.3, 184.9 and 246.6 µg/L) of PAT for 2 hours.

57. For the determination of DNA strand breaks and oxidative DNA base modifications 0.4×10^6 cells per mL were suspended in 14 mL $DMEM_{10}$ and treated with PAT (≥98.0%) or solvent (DMSO, final concentration 0.1%) for 1 hour. Post treatment, 2×10^6 cells were seeded in large cell culture flasks with 20 mL $DMEM_{10}$, and were allowed to attach for 24 hours prior to treatment with PAT or DMSO for 4 h. The alkaline filter elution assay (Kohn *et al*., 1976) was used with modifications (Epe and Hegler, 1994; Pflaum *et al*., 1997; Pflaum and Epe, 2000). After treatment, cells were harvested and placed on ice until further processing. Approximately 1.5×10^6 cells were flushed with PBSG onto a polycarbonate filter. After lysing the cells, DNA was washed with BE1 buffer, then treated with fpg protein (dissolved in BE1 buffer containing 100 µg mL^{-1} BSA) and lysed again (lysis buffer with 0.5 mg mL−1 proteinase K) followed by rinsing with BE1 buffer. DNA was eluted from the filter by 20 mL elution buffer within 8 hours. Elution buffer was collected in 11 fractions. Elution buffer containing the DNA was neutralized and DNA content in the fractions and on the filter measured by fluorescence after staining with Hoechst 33258. The sum of DNA modifications sensitive to repair endonucleases and DNA strand breaks (including DNA single- and double-strand breaks as well as alkali-labile sites) was obtained from experiments in which the cellular DNA was incubated for 60 minutes at 37°C with the repair endonuclease (fpg protein). The numbers of modifications incised by the repair endonuclease were obtained by subtraction of the number of DNA strand breaks observed in experiments without endonuclease treatment. Elution curves obtained with -irradiated cells were used for calibration, assuming that 6 Gy generates 1 strand break/106 bp (Kohn *et al*., 1976). As a positive control, visible light was used to induce oxidative DNA modifications (Pflaum *et al*., 1998). Cells were irradiated on ice for 10 minutes with 1.5 kJ energy using a Turbo Lux Profi lamp attached with a maxi soft compact.

58. Two methods were used to determine DNA cross linking. The first was by alkaline filter elution (AFE). DNA–DNA crosslinks by AFE were determined as described by Batel *et al*. (1993). Briefly, the method is similar to the determination of DNA strand breaks but, in part, with different buffers. DNA was treated with bleomycin-Fe(II) complex. Ten µL of this solution were then mixed with 35 mL washing solution and 3 mL of this mixture were pipetted onto the DNA within 10 min (equivalent of approximately 0.43 IE). After another washing step, DNA was eluted and quantified as described above. Cross linking agents reduce the measurable number of strand breaks induced by bleomycin (Kohn, 1991). For the second method DNA–DNA cross-links by ethidium bromide fluorescence assay was carried out. The V79 cells were seeded in large cell culture flasks (2×10^6 cells, 20 mL $DMEM_{10}$) and were allowed to attach and resume proliferation for 24 hours prior to treatment with solvent (0.1% DMSO), MMC, or PAT for 1–24 hours. Subsequently, DNA–DNA crosslinks were determined by ethidium bromide fluorescence as described by de Jong *et al*. (1986). Briefly, cells were harvested, washed with PBS-CMF and lysed overnight at 37˚C in a shaking water bath. Then, heparin was added and after another 20 min at 37°C, staining solution was added. Fluorescence was measured before and after denaturization of the DNA in boiling water for 5 minutes followed by rapid cooling to room temperature using a RF1501 spectrofluorimeter.

The ratio between the two measurements relative to the ratio of solvent control is indicative of cross-linked DNA as described elsewhere (de Jong *et a*l., 1986).

59. The study reported no increase of DNA strand breaks or fpg-sensitive sites was observed at concentrations of PAT up to 10 µM (1541.2 µg/L). Only treatment with concentrations from 20–50 µM (3082.4- 7706 µg/L) PAT resulted in an increase of total DNA strand breaks and fpg-sensitive sites. Similar effects as observed after treatment with PAT for 1 hour were seen after treatment of V79 cells with PAT for 4 hours. Treatment with 0.4–2.4 µM (61.6- 369.9µg/L) demonstrated no induction of total DNA strand breaks or fpg-sensitive sites was observed. Treatment of V79 cells with 0.75 and 1.5 µM (115.59 and 231.18 µg/L) PAT significantly reduced the number of visible light-induced strand breaks from 6.6±0.5 modifications per 10^6 base pair (bp) to 4.4 ± 1.8 modifications per 10^6 bp. The authors indicated that these findings are indicative of the induction of DNA–DNA interstrand cross-links. Furthermore, the authors stated that cross-links formed by 1.5 µM PAT appeared to plateau after 12 hours.

60. Schumacher *et al*., 2005 also demonstrated results that PAT causes mutations at the hypoxanthine guanine phosphoribosyl transferase (HPRT) locus in cultured Chinese hamster V79 cells. V79 cells were treated with PAT (≥98.0%) (0,0.1,0.5,0.65,0.8,1.0, 1.5, 2.0 and 2.5 µM-0, 15.4, 77.06, 100.2, 123.3, 154.12, 231.2, 308.2 and 385.3 µg/L) for 24 hours. Cells were fixed and then a standard HPRT assay was carried out. For the determination of cell cycle distribution cells were fixed post treatment of PAT (0, 0.3, 0.6, 0.9 and 1.2 µM0, 46.2, 92.5, 138.7 and 184.944 µg/L) and stained with CyStain DNA Protein 2 staining solution. Measurement was performed with a PA II flow cytometer. For the microscopic discrimination between G2 and M phase chromosomes, nuclei were stained with DAPI/antifade and the cytoplasmic microtubule complex and mitotic spindles were stained with anti-α-tubulin antibodies for the scoring of mitotic cells and freshly divided cells as described in Lehmann and Metzler (2004). Scores of two experiments were added and statistically analysed by the chi-square test.
The effect of PAT on the cell cycle was seen by incubation with PAT (0, 0.3, 0.6, 0.9 and 1.2 µM-0, 46.2, 92.5, 138.7 and 184.944 µg/L) for 24 hours which saw an increase of cells in G2/M phase. The proportion of cell in G2/M phase of cycle increased continually during the first 4.5 hours of PAT exposure. During this interval virtually no cells were able to enter G1/G0 phase, but G1/G0 passed into S phase without interference, resulting in the almost complete disappearance of the G1/G0 peak after 4.5 hours treatment with PAT (Fig. 10 and Fig. 11). The spontaneous frequency of HPRT mutations in the V79 was 7.5 ± 6 per 10^6 viable cells. A concentration dependent increase of the mutation frequency was also observed after incubation with PAT for 2 hours, which was already statistically significant for a concentration of 0.5 µmol L^{-1} (Fig. 12 and Fig. 13). A statistically significant increase of the mutation frequency was observed even with 0.3 µmol L^{-1} PAT in cells. The authors stated that when GSH depleted cells were exposed to PAT, the mutation frequency was elevated by a factor of ~3 compared to cells with normal GSH level.

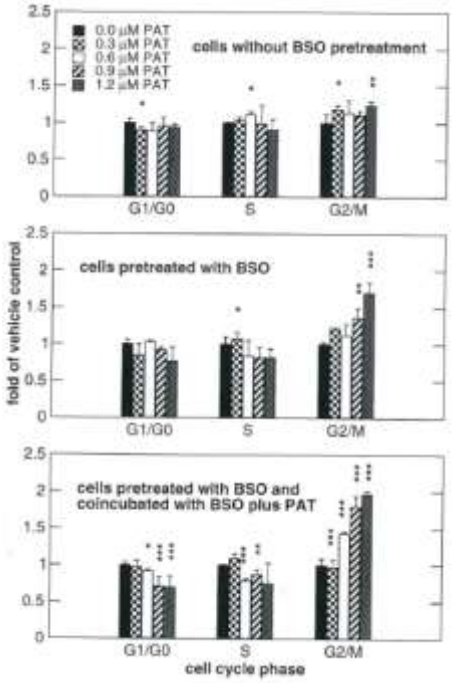

Figure 10. Effect of PAT on cell cycle distribution in cultured V79 cells. Cell with normal GSH level (*top*) and cells with reduced GSH level (*centre*) were incubated with different concentration of PAT for 24 hours. In a third experiment, cells with reduced GSH level were coincubated with PAT and 20µmol L^{-1} BSO for 24 h (*bottom*). Data are expressed as multiples of values for vehicle controls in each phase of the cell cycle and represent means from four independent incubations ± standard deviation. *Asterisks* indicate significant differences from the corresponding cell-cycle phase in the vehicle control. Levels of significance: * $P<0.05$, **, $P<0.01$; ***, $P< 0.005$. (Figure taken from Schumacher *et al*., 2005).

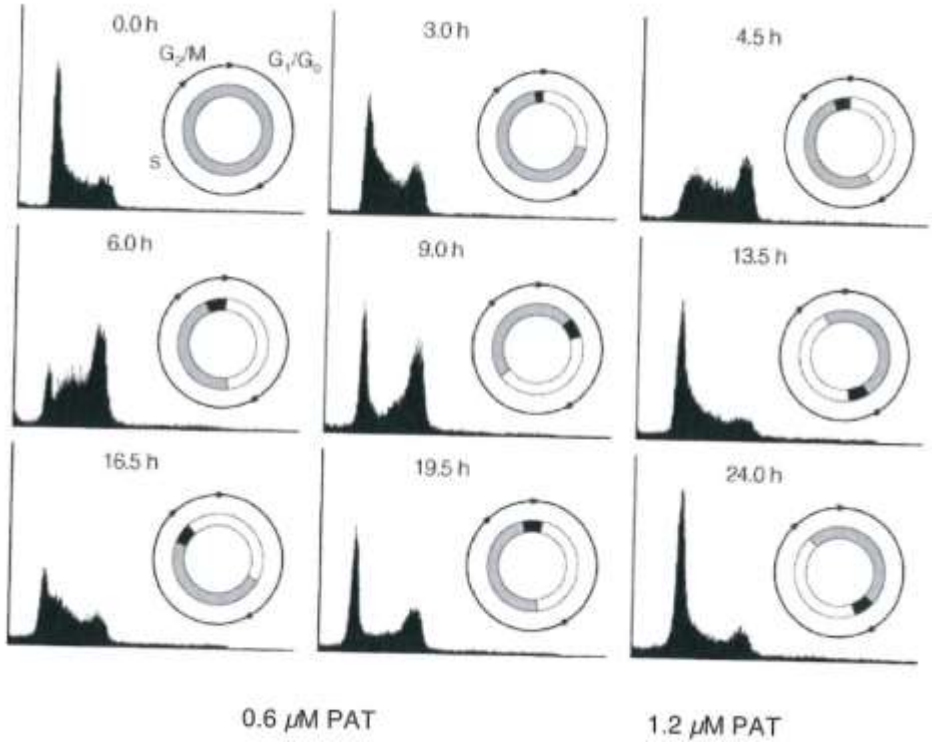

Figure 11. Cell cycle analysis of V79 cells after PAT treatment (0-24 hours). Cell cycle distribution was determined at the beginning of treatment (0 hr) and every 1.5 hrs during the treatment period. One complete turn of the circle represents the completion of one cell cycle (approximately 11 hours). *Arrow heads* mark transitions between cell cycle phases. *Grey*, unsynchronized cell population, *white*, no cells, black, accumulation of partially synchronized cells as described in the text. (Figure taken from Schumacher *et al*., 2005).

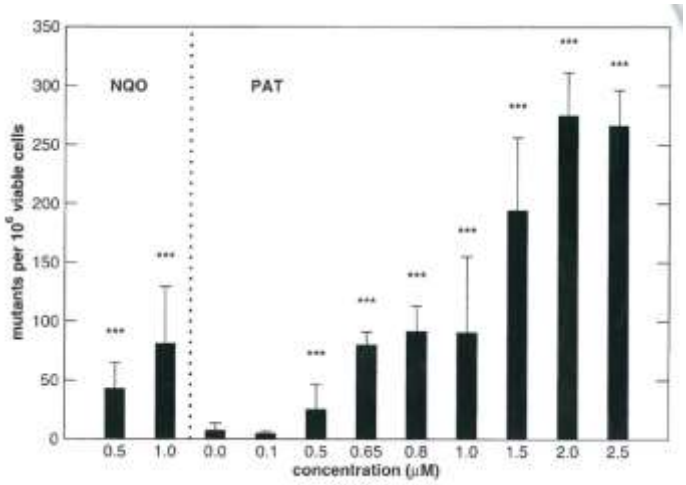

Figure 12. Frequency of mutations at the HPRT gene locus in V79 cells with different concentrations of PAT. Data represent means of two to four independent experiments ± standard deviation. *Asterisk*s indicate significant differences from the corresponding vehicle controls. Levels of significance ***, *P* <0.005. (Figure taken from Schumacher *et al*., 2005).

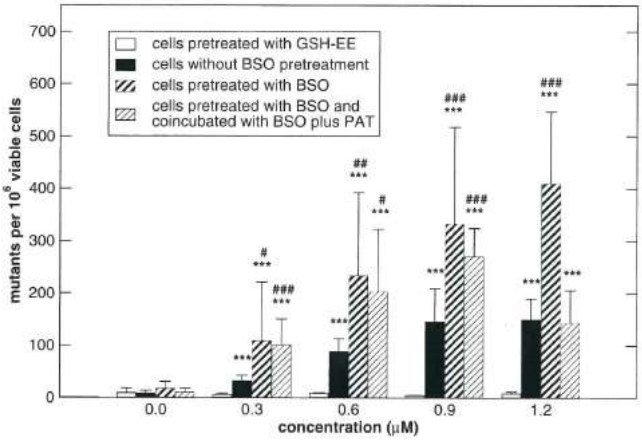

Figure 13. Frequency of mutations at the HPRT gene locus in cultured V79 cells with normal GSH level, with reduced GSH level and with increased GSH level after treatment with different concentrations of PAT for 24 hours. Cells were pre-treated with 20 µmol L^{-1} BSO to reduce the GSH level and then incubated with PAT or cells were pre-treated with BSO and then co-incubated with 20 µmol L^{-1} BSO and PAT for 24 hours. To elevate GSH levels cells were pre-treated with 17mmol L^{-1} GSH EE for 2.5 hours. Data represent means from three independent experiments ± standard deviation. *Asterisks* indicate significant differences from the corresponding vehicle control with same GSH level. *Hash signs* indicate significant differences from the corresponding treatment in cells with normal GSH level. Levels of significance: */#, *P*< 0.05; **/, *P*<0.01; ***/###, *P*<0.005 (Figure taken from Schumacher *et al*., 2005).

61. Ayed- Boussema *et al.,* 2011 study used hepatoma cell line (HepG2) cells to demonstrate p53 expression and chromosome aberrations induced by PAT. DNA damage was detected by assessing comet and chromosome aberration assays. Single cell electrophoresis *i.e.* comet assay was used to detected cellular lesions/ genotoxicity after HepG2 cells were exposed to PAT 15 µM (2311.8 µg/L) for 24 hours (~300 DNA damage score). In the chromosome aberration assay, HepG2 cells were exposed to PAT 15 µM (2311.8 µg/L) for 24 hours. Percentages values of structural aberrations with special emphasis on gaps, rings, breaks and centric fusions are presented in Table 6, below.

Table 6. Percentage of different types of chromosome aberrations observed post PAT exposure. (Table taken from Ayed- Boussema *et al.,* 2011).

	Centric fusion	Break	Ring	Gap	Total
Control	4.33 ± 1.5	3 ± 1	0 ± 0	0 ± 0	7.3 ± 1.5
PAT 15 µM	11 ± 1	17 ± 2	3.33 ± 0.58	4.33 ± 0.58	35.7 ± 1.15[a]

Three hundred metaphases were examined per treatment (100 metaphases/treatment/experiment)
Data are presented as Mean ± S.D.
[a] Statistically significant from the control at *P* <0.05

62. In another experiment the authors stated that significant p53 induction post PAT exposure (15 µM- 2311.8 µg/L) for 24 hours was demonstrated via western blotting (standard as described above in other experiments) and quantified by scanning densitometry (Figure 13).

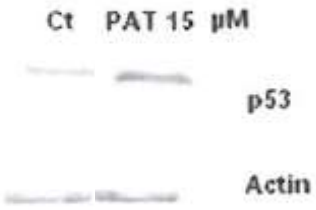

Densitometry Control ~200 PAT 15 ~600* * statistically different from control *P* <0.05

Figure 13. Western blot analysis of cells exposed to PAT (15µM) for 24 hours. (Figure taken from Ayed- Boussema *et al.,* 2011)

63. In addition, the authors stated that it is important to note that when they simultaneously exposed Vitamin E and PAT together it caused significant reduction in DNA fragmentation in a concentration dependent manner, in which they suggest an anticlastogenic effect by scavenging free radicals.

64. Wu *et al.* (2005) study explored the role of ERK1/2 activation in PAT-induced DNA damage, phosphorylation of ERK1/2 contribution to DNA damage induced by PAT through various experiments described below. HEK293 cells were left untreated or treated with 10 µM U0126[12] for 30 minutes before co-exposure to PAT (7.5 and 15 µM- 1155.9 and 2311.8 µg/L) or H_2O_2 (15 µM; positive control) for 1 hour, and then subjected to standard SCGE assays. When HEK293 cells were treated with 7.5 µM (1155.9 µg/L) PAT alone, the tail moment value (3.93 ± 0.33) was approximately twice that in the untreated control (1.99 ±0.3) and this value was reduced to 2.19 ±0.47 in the presence of U0126 (Figure 14). A similar effect was observed in 15 µM PAT-treated cultures. In contrast, U0126 did not influence the tail moment values induced by 15 µM H_2O_2. These results suggest that activation of the ERK1/2 pathway is involved in the PAT-induced DNA damage.

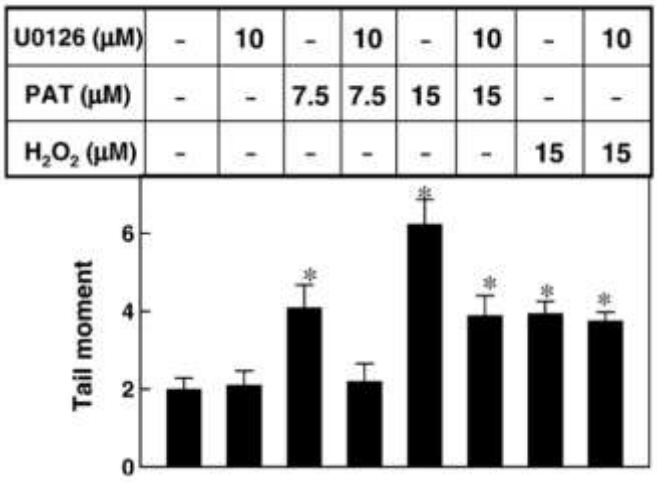

Figure 14. Effect of U0126 on PAT-induced DNA damage in HEK293 cells. HEK293 cells were left untreated or treated with 10 µM U0126 for 30 min and then co-

[12] U0126: highly selective inhibitor of both MEK1 and MEK2, a type of MAPK/ERK kinase

incubated with vehicle (15% ethanol in PBS), PAT (7.5 or 15 µM-1155.9 and 2311.8 µg/L), or H_2O_2 (15 µM-2311.8 µg/L) for 1 hour. DNA damage levels, expressed as the tail moment value, were determined using the SCGE assay. The data are expressed as the mean ± SEM (*n* = 6). *Significant difference (*P* < 0.05) compared to the control group treated with neither PAT nor U0126 (Figure taken from Wu *et al.,* 2005).

65. The role of ERK1/2 activation in DNA synthesis in PAT treated cells was also studied using the Bromodeoxyuridine / 5-bromo-2'-deoxyuridine (BrdU[13]) incorporation assay. BrdU incorporation of HEK293 cells was significantly reduced to 72 and 64% of control levels following 24 hours treatment with 0.3 or 0.5 µM (46.236-77.06 µg/L) PAT, respectively (Figure 15). Coadministration of U0126 with PAT did not elevate or reduce BrdU levels in PAT-treated cultures. The authors stated that these data suggest that activation of the ERK pathway in PAT-treated HEK293 cells does not directly correlate with the cytotoxicity or DNA synthesis rate in PAT-treated HEK293 cells.

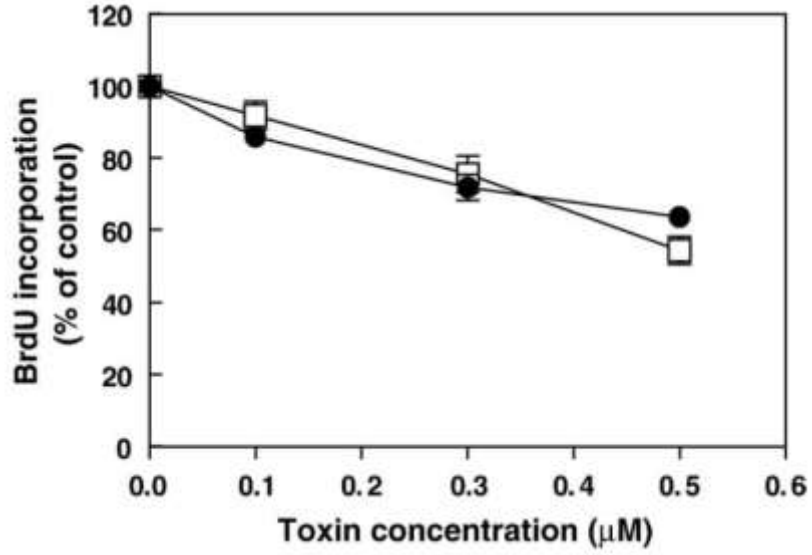

Figure 15. Effect of U0126 on DNA synthesis in PAT-treated HEK293 cells. HEK293 cells were left untreated (•) or treated with 10 µM U0126 for 30 min (□) and then co-incubated for another 24 hours with the same agents plus vehicle or various concentrations of PAT (0.1, 0.3, or 0.5 µM). DNA synthesis levels were measured using the BrdU incorporation assay and expressed as a percentage of that in control cells exposed to vehicle only. The data are given as the mean ± SEM (n = 4) (Figure taken from Wu *et al.,* 2005).

66. To identify the downstream target genes activated via the PAT-induced ERK1/2 pathway, RNA preparations from HEK293 cultures treated with 15 µM PAT or vehicle for 90 minutes were subjected to cDNA microarray analysis. a significant upregulation of early growth response gene 1 (*egr-1*) mRNA levels was seen in PAT-treated cells, whereas levels of transcripts corresponding to *c-fos*, *fos B*, *JunB* or the house-keeping gene *gapd* (glyceraldehyde-3-phosphate dehydrogenase) were not affected compared to solvent-treated cultures (Fig. 16).

[13] Bromodeoxyuridine: a synthetic nucleoside that is an analog of thymidine. BrdU is commonly used in the detection of proliferating cells in living tissues. 5-Bromodeoxycytidine is deaminated to form BrdU.

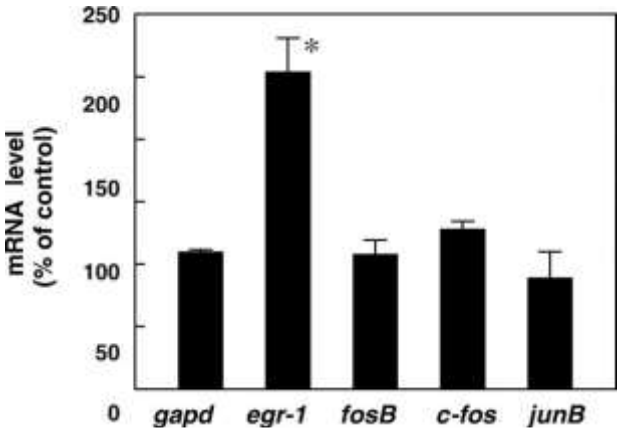

Figure 16. Induction of *egr-1* gene expression by PAT in HEK293 cells. HEK293 cultures with 80% confluence were treated with vehicle (15% ethanol in PBS) or 15 µM PAT for 90 min, and then total RNA was extracted and subjected to cDNA microarray analysis. The data are expressed as the mean ± SEM for two independent experiments. *Significant difference compared to *gapd* mRNA levels ($P < 0.05$) (Figure taken from Wu *et al.,* 2005).

67. Since PAT treatment induced ERK1/2 phosphorylation in HEK293 cell cultures, its effect was also examined in human peripheral blood mononuclear cells (PBMCs) and in Madin-Darby Canine Kidney (MDCK) cells. When freshly prepared human PBMCs were treated with various concentrations of PAT for 30 min, dose-dependent ERK1/2 phosphorylation was observed (Fig. 17). Similarly, in MDCK cells, PAT concentrations equal to or higher than 15 µM (2311.8 µg/L) resulted in a marked increase in phospho-ERK1/2 levels; this effect was inhibited in the presence of U0126 or PD98059.

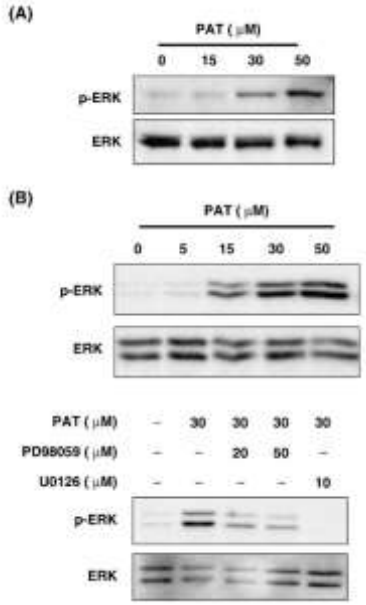

Figure 17. Activation of ERK1/2 by PAT in human PBMCs (A) and MDCK cells (B). The cells were treated for 30 min with various concentrations of PAT (0–50µM) and then ERK1/2 activation in whole cell extracts was determined by Western blotting using anti-phospho-ERK1/2 antibodies. In the lower panel of (B), MDCK cells were pre-treated for 30 minutes without or with inhibitors and then co-incubated with the

same agent plus vehicle or 30 µM PAT for another 30 minutes before cell extract preparation and Western blot analysis (Figure taken from Wu *et al.,* 2005).

Wu *et al*., 2008 further demonstrated effects of PAT on DNA fragmentation. Exposure of HL-60 cells to PAT (≥98%) at 1.0 and 2.5 µM (154.12 and 385.3 µg/L) showed the phenomenon of nuclear fragmentation and chromatin condensation to 2.1 ± 0.1% and 23.7 ± 3.7% of the cultures, respectively using DAPI staining (Fig. 18).

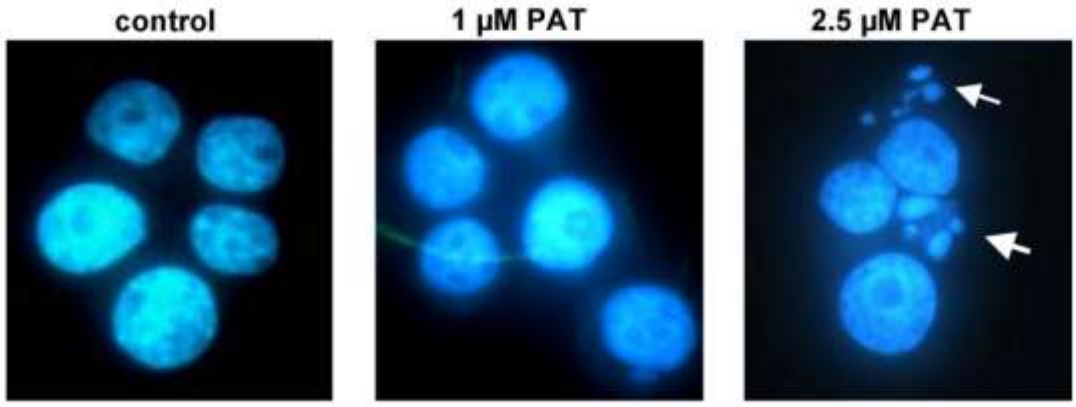

Figure 18. HL-60 cells exposed to solvent, 1 µM or 2.5 µM PAT for 6 hours were directly observed under phase-contrast light microscope with 400 X magnification and subjected to DAPI staining (Figure taken from Wu *et al* 2008).

68. To evaluate potential apoptotic DNA fragmentation, DNA was prepared from vehicle- and PAT-treated cultures and resolved by conventional agarose gel electrophoresis (Fig. 19) HL-60 cultures that were exposed to PAT exhibited the characteristic dose-dependent DNA laddering effect.

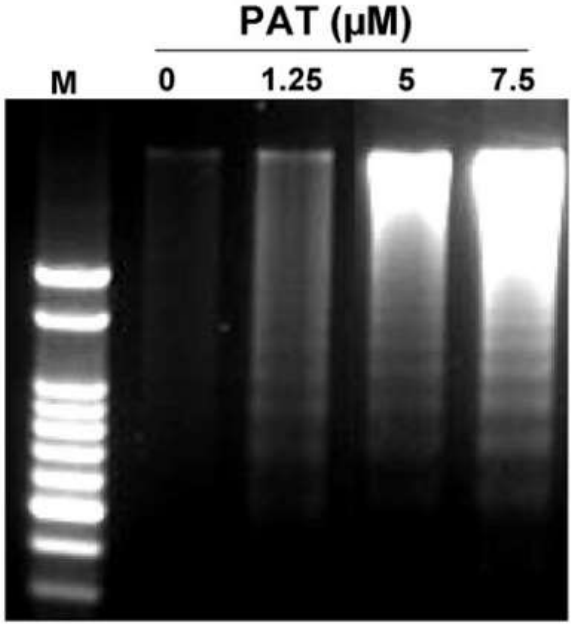

Figure 19. DNA was extracted from PAT-treated HL-60 and analyzed by 1.5% agarose gel electrophoresis. M represents the 100 bp DNA marker. Results are a representative of three separate experiments (Figure taken from Wu *et al* 2008).

When flow cytometry was adopted to quantitate the apoptotic cells in toxin-treated HL-60 cells, a hypodiploid DNA peak was observed following treatment with PAT at concentrations above 1.25 µM (192.65 µg/L) (Fig. 20). The proportion of cells in the sub-G1 phase increased from 17.4 to 43.2% following exposure to 1.25 (192.65 µg/L) and 5 µM (770.6 µg/L) of PAT.

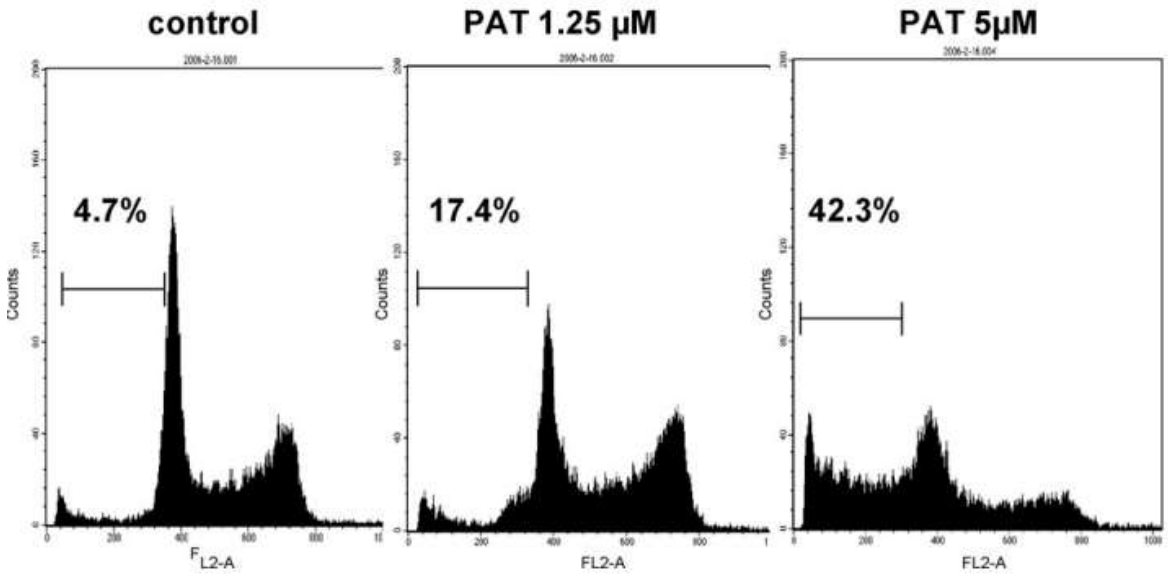

Figure 20. HL-60 cells exposed to solvent, 1 µM or 2.5 µM PAT for 6 h and were fixed and stained with propidium iodide (PI). The percentage of cells within the hypodiploid DNA region was determined by flow cytometry. Results are a representative of three separate experiments (Figure taken from Wu *et al* 2008).

69. Zhang *et al*. (2015) demonstrated that when HEK293 cells were exposed to 5, 10 and 15 µM (770.6, 1541.2 and 2311.8 µg/L) PAT (≥99%) for 8 hours, approximately 90% of cells showed chromatin condensation, nuclear fragmentation and high acridine orange[14] (AO) signals. Moreover, cells were stained with Hoechst 33342 for nuclei observation, the number of apoptotic cells with shrunken and irregular shape or degradation with aggregation and fragmentation of chromatin significantly increased with PAT treatment (Fig.21).

[14] Acridine orange: used as a nucleic acid-selective fluorescent cationic dye useful for cell cycle determination. Being cell-permeable, it interacts with DNA and RNA by intercalation or electrostatic attractions respectively

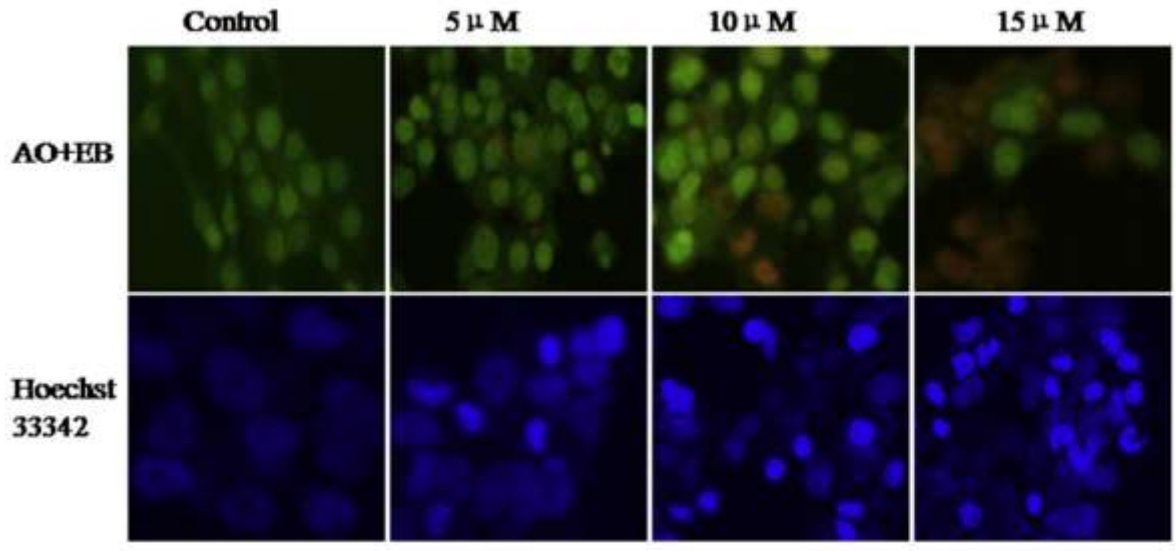

Figure 21. PAT induces apoptosis in HEK293 cells. Cells were seeded at a density of 1 x 10^5 cells/mL in 96-well polystyrene culture plates at 37°C with 5% (v/v) CO_2 for one day. After 24 hours of incubation, cells were incubated with variable concentrations of PAT for 8 hours, and then exposed to 10 mg/mL Hoechst 33342 or 100 mg/mL AO-ethidium bromide (EB). Chromatin condensation and nuclear fragmentation were considered to indicate apoptotic cells. In AO-EB experiments, green cells were counted as live cells; yellow cells were counted as early apoptotic cells; orange cells were counted as late apoptotic cells; and red cells were counted as dead cells. Scale bar = 50 μm (Figure taken from Zhang *et al,.* 2015).

In vivo

70. Gül *et al*. (2006) noted ultrastructural damage via electronic microscopy in the thymus capillary cells of rats leading to clumping of chromatin and formation of pyknotic nuclei.

71. Wister albino male rates (5-6 weeks old) were orally gavaged with 0.1 mg kg^{-1} day^{-1} of PAT (≥98%) for either 60 days (P-60 group) or 90 days (P-90 group) with a comparison group of sterile water (*n*=10 for each group). Post treatment, thymus glands were dissected and the tissues were fixed, stained with uranyl acetate and lead citrate followed by examination of transmission electron microscopy (TEM) at 80kV. The authors stated that the dose was extrapolated from estimated exposure levels for humans. Results revealed that in the P-60 group the chromatin material of endothelial nucleus was seen clumping near the nuclear envelope in the capillary wall of the thymus. Clumping of chromatin in the nucleus of smooth muscle cell and widening of the perinuclear space was also observed. In the P-90 group, nuclei had chromatin inclusions and the endothelial cells were found to have pyknotic nuclei in the capillary wall of the thymus. The authors stated that the nuclei had lost almost all of their chromatin material, but the small amount remaining was located beneath the nucleus inner membrane. The authors hypothesised that this was due to the toxic effect of PAT as a cascade effect of cell injury.

72. In the de Melo *et al.* (2012) study, male CF-1 mice were given a single dose of 1.0, 2.5 mg, or 3.75 mg/kg PAT intraperitoneally (i.p) for 3 hours. DNA-damaging

effects were tested in the brain, kidneys, liver and urinary bladder using the alkaline comet assay. The alkaline comet assay was performed in the standard way as described by Singh *et al*. (1988), with minor modifications (Collins, 2004; Tice *et al*., 2000). The cells were scored visually into five classes according to tail length: class 0: undamaged, without a tail; class 1: with a tail shorter than the diameter of the head (nucleus); class 2: with a tail length 1–2 times the diameter of the head; class 3: with a tail longer than 2 times the diameter of the head; and class 4: comets with no heads. International guidelines and recommendations for the comet assay consider the visual scoring of comets to be a well-validated evaluation method (Burlinson *et al*., 2007). The genotoxic effects were estimated based on two different parameters: the damage index (DI) and the damage frequency (DF). The damage index ranged from 0 (completely undamaged: 100 cells 0) to 400 (with maximum damage: 100 cells 4). The damage frequency (%) was calculated based on the number of cells with tails compared to the number of cells with no tail. The vehicle was used as a negative control, and treatment with 4 x 10^5 M methyl methanesulphonate (MMS) was used as a positive control.

73. The DI values were as follows: in hippocampus increased from 36.2 in control animals to 127.5, liver (44.3–138.4) and kidneys (31.5–99); decreased levels of GSH (hippocampus – from 46.9 to 18.4 nmol/mg protein); and an increase in lipid peroxidation (hippocampus – from 5.8 to 20.3 malondialdehyde (MDA) equivalents/mg protein). A statistically significant, dose-dependent increase in DI was observed in the brain, liver and kidneys of mice exposed to 2.5 (hippocampus $p < 0.05$; cortex, bulb, cerebellum, kidney and liver, $p < 0.01$) and 3.75 mg/kg b.w. (hippocampus, bulb, cerebellum and liver, $p < 0.001$; cortex and kidney, $p < 0.01$) PAT. In contrast, no significant DNA damage was observed in the urinary bladder at any tested dose. The authors stated that the regions of the brain tested were found to exhibit the highest level of DNA damage. They noted that the brain is the primary target organ for PAT-induced DNA damage because it shows the greatest severity of lesions, however the authors noted that this is from i.p exposure, the oral route is closer to the real exposure scenario since PAT is mainly found in contaminated food.

74. In the Song *et al.* study (2014) the authors aimed to evaluate the genotoxicity of PAT in bone marrow and investigate the protective effect of green tea polyphenol (GTP) at three different doses (25, 50 and 100 mg/kg bw/day) against damages occurred by PAT. Groups of 6 experimental male kumming mice received daily i.p. injection of PAT (≥98%) (1 mg/kg) for 7 days. Bone marrow cells were harvested, and a bone marrow micronucleus test / bone marrow chromosomal aberration test was carried out. For the bone marrow micronucleus test, bone marrow cells were centrifuged at 1200 rpm/10 min and the pellet was re-suspended in 0.56% KCl solution and incubated at 37°C for 25 min. Cells were re-centrifuged at 1200 rpm/10 min and fixed in cold Carnoy's fixative three times. Cells were spread on a slide by pulling one drop of bone marrow suspension behind a cover glass held at a 45°. Smears were air-dried, fixed in methanol and stained with May-Grünwald/Giemsa and evaluated with a fluorescence microscope. One thousand erythrocytes were observed from each animal to determine micronuclei in polychromatic erythrocyte (MNPCE,), micronuclei in normochromatic erythrocytes (MNNCE,) and polychromatic erythrocyte/polychromatic erythrocyte + normochromatic erythrocyte in 1000 cells [PCE / 1000 (PCE + NCE)]. PAT was found to induce micronucleus and chromosomal aberration formation nuclei in polychromatic erythrocytes (MNPCE)

and micronuclei in normochromatic erythrocyte (MNNCE). PAT-treatment induced a significant increase in chromosomal gaps and breaks in mice bone marrow cells (p< 0.001 and p< 0.001 respectively) (Fig. 22 and Fig. 23).

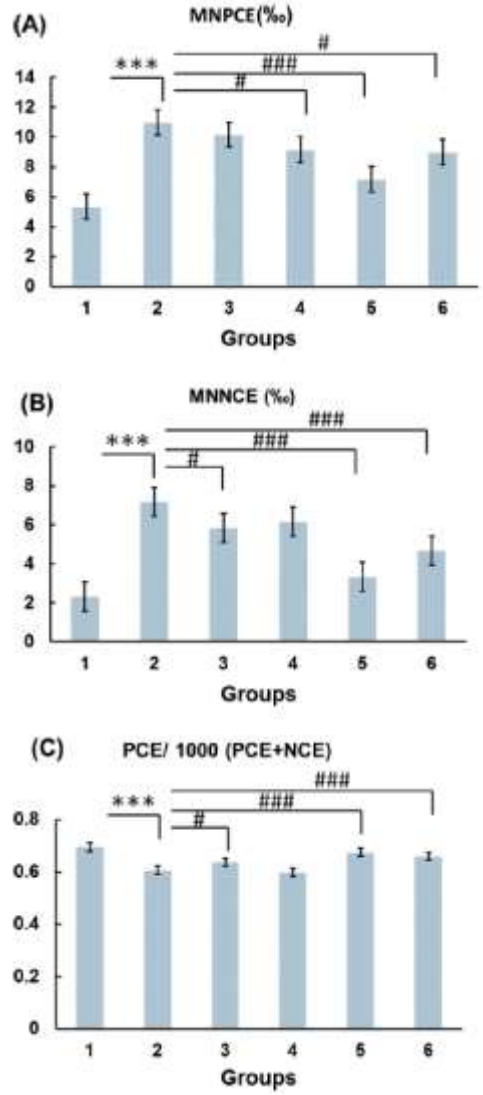

Figure 22. The effect of GTP on the induction of micronuclei in mice bone marrow cell in PAT-intoxication mice. Group 1: vehicle control, received 0.1% DMSO in saline (2 ml/kg bw/d). Group 2: received PAT (1 mg/kg). Group 3: received PAT (1 mg/kg) and GTP (25 mg/kg bw/d). Group 4: received PAT (1 mg/kg) and GTP (50 mg/kg BW/d). Group 5: received PAT (1 mg/kg) and GTP (100 mg/kg bw/d). Group 6: received PAT (1 mg/kg) and silymarin (100 mg/kg bw/d). (A), MNPCE, micronucleiin polychromatic erythrocytes. (B) MNNCE, micronuclei in normochromatic eryth-rocyte. (C), PCE/1000 (PCE + NCE), polychromatic erythrocyte/polychromatic eryth-rocyte + normochromatic erythrocyte in 1000 cells. Data are presented as the means ± S.D., n=6. *p< 0.05 or ***p< 0.001 vs control group, #p< 0.05 or ### p< 0.001 vs PAT group. (Figure taken from Song *et al* 2014).

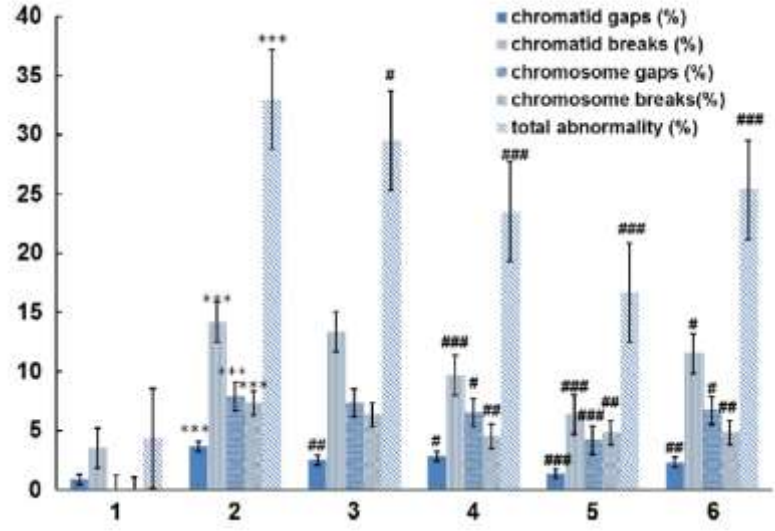

Figure 23. The effect of GTP on chromosome aberrations in mice bone marrow cell in PAT-intoxication mice. Group 1: vehicle control, received 0.1% DMSO in saline (2 mL/kg BW/d). Group 2: received PAT (1 mg/kg). Group 3: received PAT (1 mg/kg) and GTP (25 mg/kg BW/d). Group 4: received PAT (1 mg/kg) and GTP (50 mg/ kg BW/d). Group 5: received PAT (1 mg/kg) and GTP (100 mg/kg BW/d). Group 6: received PAT (1 mg/kg) and silymarin (100 mg/kg BW/d). Data are presented as the means ± S.D., $n = 6$. ***$p < 0.001$ vs control group. #$p < 0.05$, ##$p < 0.01$ or ###$p < 0.001$ vs PAT group. (Figure taken from Song *et al* 2014).

Other studies

75. In other studies, Saxena *et al* (2009) demonstrated an *in vivo* topical application of PAT (≥98%) (160 µg/100 µl acetone) for 24–72 hours caused DNA damage in skin cells showing significant increase (34–63%) in olive tail moment, a parameter of comet assay and significant G1 and S-phase arrest along with induction of apoptosis (2.8–10 folds) as shown by annexin V and PI staining assay through flow cytometer.

76. Six to seven weeks old female Swiss albino mice (18–22 g) were divided into four groups. One of the groups served as control, which remained untreated. Remaining groups were treated in the following manner (i) acetone (100 µl) was topically applied for 24 h, which served as negative control; (ii) benzo(a)pyrene (BP), (160 µg/100 µl acetone) was topically applied for 24 hours and served as positive control; (iii) PAT (160 µg/100 µl acetone) was topically applied and animals were euthanized after 6, 12, 24, 48, and 72 hours.

77. Skin samples from all the groups of animals were dissected out and the single cell suspension was prepared as described earlier (Das *et al*., 2005). The alkaline comet assay technique of Singh *et al*. (1998) and Tice *et al*. (2000) was utilized for evaluation of DNA damage in mouse skin cells. Slides were prepared and scored with an image analysis system (Kinetic Imaging) attached to a fluorescence microscope equipped with appropriate filters. The microscope was connected to a computer through a charge coupled device (CCD) camera to transport images to software (Komet 5.0) for analysis. The final magnification was 400×. The parameters

undertaken in the study were the olive tail moment (OTM) (arbitrary units), tail DNA (%), and tail length (migration of the DNA from the nucleus; µm).

78. PAT treatment for 24–72 hours caused significant enhancement of OTM (34–63%), tail DNA (32–151%), and tail length (35–124%) when compared to control. However, no DNA damage was observed at 6 and 12 hours exposure of cells with PAT. PAT treatment at 6 and 12 hours did not show significant difference in percentage of cell in OTM category of 15 and 20. The DNA from skin cells prepared from PAT treated animals showed typical formation of comet.

Method of action hypothesis

79. It has been surmised that these genotoxic effects might be related to PATs ability to react with sulfhydryl groups and to induce oxidative damage (Liu *et al*., 2007; Riley *et al*., 2001).

Summary/Conclusions

80. A summary table of all the studies elucidated in this paper can be found in ANNEX A.

81. There are numerous scientific studies with evidence of PAT being genotoxic *in vitro*.

82. PAT caused DNA single-strand breaks in living cells of the bacteria *Escherichia coli* at a concentration of 10 µg/ml for 60 min. At 50 µg/ml for 60 minutes, double-strand breaks were also observed (Lee, K.S. and Röschenthaler 1986). PAT treatment (24 hours) resulted in a concentration-dependent (0,5,7,9 µM-770.6, 1078.8, 1387.08 µg/L) reactive oxygen species (ROS) generation accompanied by DNA damage (increase of DNA damage marker H2AX phosphorylation) and p53 activation evidenced by induction of its transcriptional targets Bax and p21 in Human Embryonic Kidney (HEK) 293 cells (Jin *et al*., 2016). Alves et al., (2000) demonstrated induction of chromosomal aberrations and the formation of micronucleus due to PAT 0.35–0.95µM (53.9- 146.4µg/L) *in vitro*. With respect to DNA damage effects of PAT on human lymphocytes, PAT induced a statistically significant concentration-dependent increase in the number of BN cells with NPBs in human lymphocytes. PAT was found to induce nucleoplasmic bridges (NPBs) at 5.0 and 7.5 µM (770.6- 1155.9 µg/L) concentrations (P<0.05). PAT induced a statistically significant concentration-dependent increase in the number of binucleated cells with NPBs in human lymphocytes, at least at between 5 and 7.5 µM (770.6- 1155.9 µg/L) (Donmez *et al*., 2013). In another study using the SCGE assay with HEK293 cells that were treated with PAT (5, 10, 15, 20 µM-770.6, 1541.2, 6935.4 and 3082.4 µg/L) for 2 hours demonstrated DNA damage on a single cell basis (Liu *et al*., 2003).

83. In contrast, Schumacher *et al* (2006) study reported no increase of DNA strand breaks or fpg-sensitive sites was observed up to concentrations of PAT up to 10µM PAT. Only treatment with concentrations from 20–50 µM PAT resulted in an increase of total DNA strand breaks and fpg-sensitive sites. Similar effects as

observed after treatment with PAT for 1 hour were seen after treatment of V79 cells with PAT for 4 hours. Treatment with 0.4–2.4 µM (61.6-369.9 µg/L) of PAT demonstrated no induction of total DNA strand breaks or fpg-sensitive sites was observed.

84. *In vivo* studies such as Gül *et al*. (2006) noted ultrastructural damage via electronic microscopy in the thymus capillary cells of rats leading to clumping of chromatin and formation of pyknotic nuclei due to PAT exposure (0.1 mg kg^{-1} day^{-1} for 60 days). Another study demonstrated a statistically significant, dose-dependent increase in DI was observed in the brain, liver and kidneys of mice exposed to 2.5 and 3.75 mg/kg PAT i.p. for 3 hours de Melo *et al.* (2012) study.

85. In addition, it is important to note that various studies look at simultaneously exposing antioxidants *e.g.* Vitamin E and PAT together which caused significant reduction in DNA fragmentation in a concentration dependent manner, in which they suggest an anticlastogenic effect by scavenging free radicals.

QUESTIONS FOR THE COM

The COM are asked to comment on the genotoxicity studies provided.

i) Has an appropriate range of studies been conducted to come to a conclusion on the genotoxic potential of PAT?
ii) If not are there any specific studies which need to be undertaken to provide the necessary information?
iii) Do Members have any other comments?

Secretariat

September 2019

Abbreviations

AO	acridine orange
ALT	aminotransferase
AST	aspartate transaminase
bp	base pair
CAEG	chromosomal aberrations excluding gaps
CBMN Cyt	cytokinesis-block micronucleus cytome
COT	The Committee on Toxicity of Chemicals in Food, Consumer Products and the Environment
CONTAM	Contaminants in the Food Chain
DI	damage index
EB	ethidium bromide
EFSA	European Food Safety Authority
H_2O_2	hydrogen peroxide
HEK	human embryonic kidney
HPRT	hypoxanthine guanine phosphoribosyl transferase
i.p	intraperitoneally
JECFA	Joint FAO/WHO Expert Committee on Food Additives
MDCK	Madin-Darby Canine Kidney
MDA	malondialdehyde
MN	micronucleus
MNPCE	polychromatic erythrocytes
MNNCE	normochromatic erythrocyte
NPBs	nucleoplasmic bridges
PAT	patulin
PBMC	peripheral blood mononuclear cells
PBS	phosphate-buffered saline
PMTWI	provisional maximum tolerable weekly intake
PMTDI	provisional maximum tolerable daily intake
ROS	reactive oxygen species
SACN	Scientific Advisory Committee on Nutrition
SCGE	single cell gel electrophoresis
SO_2	sulfur dioxide

References

Adams, M.H., 1959. Bacteriophages. Bacteriophages.

Alves, I., Oliveira, N.G., Laires, A., Rodrigues, A.S. and Rueff, J., 2000. Induction of micronuclei and chromosomal aberrations by the mycotoxin patulin in mammalian cells: role of ascorbic acid as a modulator of patulin clastogenicity. *Mutagenesis*, *15*(3), pp.229-234.

Al-Hazmi, M.A., 2014. Patulin in apple juice and its risk assessments on albino mice. *Toxicology and industrial health*, 30(6), pp.534-545.

Ayed-Boussema, I., Pascussi, J.M., Rjiba, K., Maurel, P., Bacha, H. and Hassen, W., 2012. The mycotoxin, patulin, increases the expression of PXR and AhR and their target cytochrome P450s in primary cultured human hepatocytes. *Drug and chemical toxicology*, 35(3), pp.241-250.

Ayed-Boussema, I., Abassi, H., Bouaziz, C., Hlima, W.B., Ayed, Y. and Bacha, H., 2013. Antioxidative and antigenotoxic effect of vitamin E against patulin cytotoxicity and genotoxicity in HepG2 cells. *Environmental toxicology*, 28(6), pp.299-306.

Batel, R., Vukmirovic, M., Bihari, N., Zahn, R.K. and Muller, W.E.G., 1993. Nonradiometric detection of DNA crosslinks in mussel hemolymph by alkaline elution. *Analytical biochemistry*, *212*(2), pp.402-406.

Barhoumi, R. and Burghardt, R.C., 1996. Kinetic analysis of the chronology of patulin-and gossypol-induced cytotoxicity *in vitro*. *Toxicological Sciences*, 30(2), pp.290-297.

Bartolomé, B., Bengoechea, M.L., Perez-Ilzarbe, F.J., Hernandez, T., Estrella, I. and Gómez-Cordovés, C., 1994. Determination of patulin in apple juice by high-performance liquid chromatography with diode-array detection. Journal of chromatography A, 664(1), pp.39-43.

Ben-Hamida, F. and Gros, F., 1971. Transcription and translation mechanisms in a «permeabilized E. coli system. *Biochimie*, 53(1), pp.71-80.

Brackett, R.E. and Marth, E.H., 1979. Ascorbic acid and ascorbate cause disappearance of patulin from buffer solutions and apple juice. *Journal of Food Protection*, 42(11), pp.864-866.

Burghardt, R.C., Barhoumi, R., Lewis, E.H., Bailey, R.H., Pyle, K.A., Clement, B.A. and Phillips, T.D., 1992. Patulin-induced cellular toxicity: a vital fluorescence study. *Toxicology and applied pharmacology*, 112(2), pp.235-244.

Burlinson, B., Tice, R.R., Speit, G., Agurell, E., Brendler-Schwaab, S.Y., Collins, A.R., Escobar, P., Honma, M., Kumaravel, T.S., Nakajima, M. and Sasaki, Y.F., 2007. Fourth International Workgroup on Genotoxicity testing: results of the *in vivo* Comet assay workgroup. *Mutation Research/Genetic Toxicology and Environmental Mutagenesis*, 627(1), pp.31-35.

Caria, H., Chaveca, T., Laires, A. and Rueff, J., 1995. Genotoxicity of quercetin in the micronucleus assay in mouse bone marrow erythrocytes, human lymphocytes, V79 cell line and identification of kinetochore-containing (CREST staining) micronuclei in human lymphocytes. *Mutation Research/Genetic Toxicology*, 343(2-3), pp.85-94.

Collins, A.R., 2004. The comet assay for DNA damage and repair. *Molecular biotechnology*, 26(3), p.249.

Countryman, P.I. and Heddle, J.A., 1976. The production of micronuclei from chromosome aberrations in irradiated cultures of human lymphocytes. *Mutation Research/Fundamental and Molecular Mechanisms of Mutagenesis*, 41(2-3), pp.321-331.

Dailey, R.E., Blaschka, A.M. and Brouwer, E.A., 1977. Absorption, distribution, and excretion of [14C] patulin by rats. Journal of Toxicology and Environmental Health, Part A Current Issues, 3(3), pp.479-489.

de Melo, F.T., de Oliveira, I.M., Greggio, S., Dacosta, J.C., Guecheva, T.N., Saffi, J., Henriques, J.A.P. and Rosa, R.M., 2012. DNA damage in organs of mice treated acutely with patulin, a known mycotoxin. *Food and chemical toxicology*, *50* (10), pp.3548-3555.

de Jong, S., Zijlstra, J.G., Timmer-Bosscha, H., Mulder, N.H. and De Vries, E.G.E., 1986. Detection of DNA cross-links in tumor cells with the ethidium bromide fluorescence assay. *International journal of cancer*, *37*(4), pp.557-561.

Das, M., Ansari, K.M., Dhawan, A., Shukla, Y. and Khanna, S.K., 2005. Correlation of DNA damage in epidemic dropsy patients to carcinogenic potential of argemone oil and isolated sanguinarine alkaloid in mice. *International journal of cancer*, *117*(5), pp.709-717.

Dean, B.J., 1984. Assays for the detection of chemically-induced chromosome damage in cultured mammalian cells. *Mutagenicity testing*, A practical approach.

Donmez-Altuntas, H., Gokalp-Yildiz, P., Bitgen, N. and Hamurcu, Z., 2013. Evaluation of genotoxicity, cytotoxicity and cytostasis in human lymphocytes exposed to patulin by using the cytokinesis-block micronucleus cytome (CBMN cyt) assay. *Mycotoxin research*, 29(2), pp.63-70.

Dönmez-Altuntaş, H., Hamurcu, Z., İmamoğlu, N. and Liman, B.C., 2003. Effects of ochratoxin A on micronucleus frequenncy in human lymphocytes. *Food/Nahrung*, 47(1), pp.33-35.

Drusch, S., Kopka, S. and Kaeding, J., 2007. Stability of patulin in a juice-like aqueous model system in the presence of ascorbic acid. Food chemistry, 100(1), pp.192-197.

Eastmond, D.A. and Tucker, J.D., 1989. Identification of aneuploidy-inducing agents using cytokinesis-blocked human lymphocytes and an antikinetochore antibody. *Environmental and molecular mutagenesis*, 13(1), pp.34-43.

Epe, B. and Hegler, J., 1994. [12] Oxidative DNA damage: Endonuclease fingerprinting. In *Methods in enzymology* (Vol. 234, pp. 122-131). Academic Press.

Fenech, M., 1993. The cytokinesis-block micronucleus technique: a detailed description of the method and its application to genotoxicity studies in human populations. *Mutation Research/Fundamental and Molecular Mechanisms of Mutagenesis*, 285(1), pp.35-44.

Fenech, M., 2000. The *in vitro* micronucleus technique. *Mutat Res* 455:81–95

Fenech, M., 2007. Cytokinesis-block micronucleus cytome assay. *Nature protocols*, 2(5), p.1084.

Frank, H.K., 1977. Occurrence of patulin in fruit and vegetables. In Annales de la Nutrition et de l'Alimentation (Vol. 31, No. 4-6, pp. 459-465).

Frank, H.K., Orth, R. and Figge, A., 1977. Patulin in Lebensmitteln pflanzlicher Herkunft. Zeitschrift für Lebensmittel-Untersuchung und Forschung, 163(2), pp.111-114.

Glaser, N. and Stopper, H., 2012. Patulin: Mechanism of genotoxicity. *Food and Chemical Toxicology*, 50(5), pp.1796-1801.

Gül, N., Özsoy, N., Osmanagaoglu, Ö., Selmanoğlu, G. and Koçkaya, E.A., 2006. Effects of patulin on thymus capillary of rats. *Cell Biochemistry and Function*: Cellular biochemistry and its modulation by active agents or disease, 24(6), pp.541-546.

Guo, X., Dong, Y., Yin, S., Zhao, C., Huo, Y., Fan, L. and Hu, H., 2013. Patulin induces pro-survival functions via autophagy inhibition and p62 accumulation. *Cell death & disease*, 4(10), p.e 822

Heinemann, B., 1971. Prophage induction in lysogenic bacteria as a method of detecting potential mutagenic, carcinogenic, carcinostatic, and teratogenic agents. *In Chemical mutagens* (pp. 235-266). Springer, Boston, MA.

Ho, Y.L. and Ho, S.K., 1981. Screening of carcinogens with the prophage λclts857 induction test. *Cancer research*, 41(2), pp.532-536.

Ianiri, G., Idnurm, A. and Castoria, R., 2016. Transcriptomic responses of the basidiomycete yeast Sporobolomyces sp. to the mycotoxin patulin. *BMC genomics*, 17(1), p.210

Jin, H., Yin, S., Song, X., Zhang, E., Fan, L. and Hu, H., 2016. p53 activation contributes to patulin-induced nephrotoxicity via modulation of reactive oxygen species generation. *Scientific reports*, *6*, p.24455.

Kawashima, L.M., Soares, L.M.V. and Massaguer, P.R.D., 2002. The development of an analytical method for two mycotoxins, patulin and verruculogen, and survey of their presence in commercial tomato pulp. *Brazilian Journal of Microbiology*, 33(3), pp.269-273.

Kohn, K.W., 1991. Principles and practice of DNA filter elution. *Pharmacology & therapeutics*, *49*(1-2), pp.55-77.

Kohn, K.W., Erickson, L.C., Ewig, R.A. and Friedman, C.A., 1976. Fractionation of DNA from mammalian cells by alkaline elution. *Biochemistry*, *15*(21), pp.4629-4637.

Krasin, F. and Hutchinson, F., 1977. Repair of DNA double-strand breaks in Escherichia coli, which requires recA function and the presence of a duplicate genome. *Journal of molecular biology*, 116(1), pp.81-98.

Lee, K.S. and Röschenthaler, R.J., 1986. DNA-damaging activity of patulin in *Escherichia coli*. *Applied and Environmental Microbiology*, 52(5), pp.1046-1054.

Lehmann, L. and Metzler, M., 2004. Bisphenol A and its methylated congeners inhibit growth and interfere with microtubules in human fibroblasts in vitro. *Chemico-biological interactions*, *147*(3), pp.273-285.

Liu, B.H., Yu, F.Y., Wu, T.S., Li, S.Y., Su, M.C., Wang, M.C. and Shih, S.M., 2003. Evaluation of genotoxic risk and oxidative DNA damage in mammalian cells exposed to mycotoxins, patulin and citrinin. *Toxicology and applied pharmacology*, *191*(3), pp.255-263.

Liu, B.H., Wu, T.S., Yu, F.Y. and Su, C.C., 2006. Induction of oxidative stress response by the mycotoxin patulin in mammalian cells. *Toxicological Sciences*, 95(2), pp.340-347.

Maidana, L., Gerez, J.R., El Khoury, R., Pinho, F., Puel, O., Oswald, I.P. and Bracarense, A.P.F., 2016. Effects of patulin and ascladiol on porcine intestinal mucosa: An ex vivo approach. *Food and Chemical Toxicology*, 98, pp.189-194.

McGrath, R.A. and Williams, R.W., 1966. Reconstruction *in vivo* of irradiated *Escherichia coli* deoxyribonucleic acid; the rejoining of broken pieces. *Nature*, 212(5061), p.534.

Miller, J.H., 1972. Experiments in molecular genetics. Cold Spring Harbor, NY: Cold Spring Harbor Lab. Press.

Mitchell, J.B., 1988. Potential applicability of nonclonogenic measurements to clinical oncology. *Radiation research*, 114(3), pp.401-414.

Mohan, H.M., Collins, D., Maher, S., Walsh, E.G., Winter, D.C., O'Brien, P.J., Brayden, D.J. and Baird, A.W., 2012. The mycotoxin patulin increases colonic epithelial permeability *in vitro*. *Food and chemical toxicology*, 50(11), pp.4097-4102.

Moses, R.E. and Richardson, C.C., 1970. Replication and repair of DNA in cells of Escherichia coli treated with toluene. *Proceedings of the National Academy of Sciences*, 67(2), pp.674-681.

McGrath, R.A. and Williams, R.W., 1966. Reconstruction in vivo of irradiated Escherichia coli deoxyribonucleic acid; the rejoining of broken pieces. Nature, 212(5061), p.534.

McKinley, E.R., Carlton, W.W. and Boon, G.D., 1982. Patulin mycotoxicosis in the rat: toxicology, pathology and clinical pathology. *Food and Chemical Toxicology*, 20(3), pp.289-300.

McKinley, E.R. and Carlton, W.W., 1980. Patulin mycotoxicosis in Swiss ICR mice. *Food and cosmetics toxicology*, 18(2), pp.181-187.

Olive, P.L., Banáth, J.P. and Durand, R.E., 1990. Heterogeneity in radiation-induced DNA damage and repair in tumor and normal cells measured using the" comet" assay. *Radiation research*, *122*(1), pp.86-94.

Pal, S., Singh, N. and Ansari, K.M., 2017. Toxicological effects of patulin mycotoxin on the mammalian system: an overview. *Toxicology Research*, 6(6), pp.764-771

Pflaum, M., Will, O. and Epe, B., 1997. Determination of steady-state levels of oxidative DNA base modifications in mammalian cells by means of repair endonucleases. *Carcinogenesis*, *18*(11), pp.2225-2231

Pflaum, M., Kielbassa, C., Garmyn, M. and Epe, B., 1998. Oxidative DNA damage induced by visible light in mammalian cells: extent, inhibition by antioxidants and genotoxic effects. *Mutation Research/DNA Repair*, *408*(2), pp.137-146.

Pflaum, M. and Epe, B., 2000. Measuring oxidative DNA damage by alkaline elution, Lunec J, Griffiths HR (eds.), Measuring *In Vivo* Oxidative Damage: A Practical Course.

Pfeiffer, E., Groß, K. and Metzler, M., 1998. Aneuploidogenic and clastogenic potential of the mycotoxins citrinin and patulin. *Carcinogenesis*, 19(7), pp.1313-1318.

Puel, O., Galtier, P. and Oswald, I., 2010. Biosynthesis and toxicological effects of patulin. *Toxins*, 2(4), pp.613-631.

Riley, R.T. and Showker, J.L., 1991. The mechanism of patulin's cytotoxicity and the antioxidant activity of indole tetramic acids. Toxicology and applied pharmacology, 109(1), pp.108-126.

Roland, J.O. and Beuchat, L.R., 1984. Biomass and patulin production by Byssochlamys nivea in apple juice as affected by sorbate, benzoate, SO2 and temperature. *Journal of Food Science*, 49(2), pp.402-406.

Rueff, J., Chiapella, C., Chipman, J.K., Darroudi, F., Silva, I.D., Duverger-van Bogaert, M., Fonti, E., Glatt, H.R., Isern, P., Laires, A. and Leonard, A., 1996. Development and validation of alternative metabolic systems for mutagenicity testing in short-term assays. *Mutation Research/Fundamental and Molecular Mechanisms of Mutagenesis*, 353(1-2), pp.151-176.

Saxena, N., Ansari, K.M., Kumar, R., Dhawan, A., Dwivedi, P.D. and Das, M., 2009. Patulin causes DNA damage leading to cell cycle arrest and apoptosis through modulation of Bax, p53 and p21/WAF1 proteins in skin of mice. *Toxicology and applied pharmacology*, *234*(2), pp.192-201.

Schumacher, D.M., Müller, C., Metzler, M. and Lehmann, L., 2006. DNA–DNA cross-links contribute to the mutagenic potential of the mycotoxin patulin. *Toxicology letters*, 166(3), pp.268-275.

Schumacher, D.M., Metzler, M. and Lehmann, L., 2005. Mutagenicity of the mycotoxin patulin in cultured Chinese hamster V79 cells, and its modulation by intracellular glutathione. *Archives of toxicology*, 79(2), pp.110-121.

Schupp, N., Kolkhof, P., Queisser, N., Gärtner, S., Schmid, U., Kretschmer, A., Hartmann, E., Oli, R.G., Schäfer, S. and Stopper, H., 2011. Mineralocorticoid receptor-mediated DNA damage in kidneys of DOCA-salt hypertensive rats. *The FASEB Journal*, 25(3), pp.968-978.

Silva, S.J.N.D., Schuch, P.Z., Bernardi, C.R., Vainstein, M.H., Jablonski, A. and Bender, R.J., 2007. Patulin in food: state-of-the-art and analytical trends. Revista Brasileira de Fruticultura, 29(2), pp.406-413.

Singh, N.P., McCoy, M.T., Tice, R.R. and Schneider, E.L., 1988. A simple technique for quantitation of low levels of DNA damage in individual cells. *Experimental cell research*, 175(1), pp.184-191.

Singh, N.P. and Stephens, R.E., 1997. Microgel electrophoresis: sensitivity, mechanisms, and DNA electrostretching. *Mutation Research/DNA Repair*, 383(2), pp.167-175.

Song, E., Xia, X., Su, C., Dong, W., Xian, Y., Wang, W. and Song, Y., 2014. Hepatotoxicity and genotoxicity of patulin in mice, and its modulation by green tea polyphenols administration. Food and *Chemical Toxicology*, 71, pp.122-127.

Surrallés, J., Xamena, N., Creus, A., Catalan, J., Norppa, H. and Marcos, R., 1995. Induction of micronuclei by five pyrethroid insecticides in whole-blood and isolated human lymphocyte cultures. *Mutation Research/Genetic Toxicology*, 341(3), pp.169-184.

Staudenbauer, W.L., 1976. Replication of Escherichia coli DNA in vitro: inhibition by oxolinic acid. *European journal of biochemistry*, 62(3), pp.491-497.

Tice, R.R., Agurell, E., Anderson, D., Burlinson, B., Hartmann, A., Kobayashi, H., Miyamae, Y., Rojas, E., Ryu, J.C. and Sasaki, Y.F., 2000. Single cell gel/comet assay: guidelines for in vitro and in vivo genetic toxicology testing. *Environmental and molecular mutagenesis*, 35(3), pp.206-221.

Wang, T.S., Hsu, T.Y., Chung, C.H., Wang, A.S., Bau, D.T. and Jan, K.Y., 2001. Arsenite induces oxidative DNA adducts and DNA-protein cross-links in mammalian cells. *Free Radical Biology and Medicine*, *31*(3), pp.321-330.

Whittaker, B.L. and Chipley, J.R., 1979. Conditions for induction of bacteriophage from lysogenic Bacillus megaterium with aflatoxin B1. *Appl. Environ. Microbiol*., 37(3), pp.554-558.

Wu, T.S., Yu, F.Y., Su, C.C., Kan, J.C., Chung, C.P. and Liu, B.H., 2005. Activation of ERK mitogen-activated protein kinase in human cells by the mycotoxin patulin. *Toxicology and applied pharmacology*, 207(2), pp.103-111.

Wu, T.S., Liao, Y.C., Yu, F.Y., Chang, C.H. and Liu, B.H., 2008. Mechanism of patulin-induced apoptosis in human leukemia cells (HL-60). *Toxicology letters*, 183(1-3), pp.105-111.

Yazici, S. and Velioglu, Y.S., 2002. Effect of thiamine hydrochloride, pyridoxine hydrochloride and calcium-d-pantothenate on the patulin content of apple juice concentrate. Food/Nahrung, 46(4), pp.256-257.

Zhang, B., Peng, X., Li, G., Xu, Y., Xia, X. and Wang, Q., 2015. Oxidative stress is involved in Patulin induced apoptosis in HEK293 cells. *Toxicon*, 94, pp.1-7.

Zhou, S.M., Jiang, L.P., Geng, C.Y., Cao, J. and Zhong, L.F., 2010. Patulin-induced oxidative DNA damage and p53 modulation in HepG2 cells. *Toxicon*, *55*(2-3), pp.390-395.

ANNEX A

COMMITTEE ON THE MUTAGENICITY OF CHEMICALS IN FOOD CONSUMER PRODUCTS AND THE ENVIRONMENT

REVIEW OF GENOTOXICITY OF PATULIN (PAT)

Table 1 summarises the genotoxic potential studies of patulin elucidated in this paper.

Table 1. Genotoxicity studies

Organism	Mode	Concentration/Treatment time	Changes in the nucleus, chromosome and gene/DNA/RNA	Reference
CF-1 mice (male)	*in vivo* i.p	1.0, 2.5 mg, 3.75 mg/kg (single dose) (3 hours)	dose-dependent increase in DNA damage was observed in the brain, liver and kidneys of mice exposed to 2.5 and 3.75 mg/kg	De Melo et al. (2012)
Kunming mice (male)	*in vivo* i.p.	1 mg/kg (24 hours)	induction micronucleus and chromosomal aberration formation nuclei in polychromatic erythrocytes (MNPCE) and micronuclei in normochromatic erythrocyte (MNNCE).	Song et al. (2012)
Wister albino male rates	*in vivo* (Oral gavage)	0.1 mg kg^{-1} day^{-1} (60 days and 90 days)	Clumping of chromatin/ formation of pyknotic nuclei	Gül et al (2006)
Chinese hamster V79 cells	*in vitro*	0.1 and 0.5 µM for (6 hours)	PAT induced MN in a concentration-dependent manner	Pfeiffer et al. (1998)
Human Embryonic Kidney (HEK) 293 cells	*in vitro*	0,5,7,9 µM (24 hours)	DNA damage (increase of DNA damage marker H2AX phosphorylation)	Jin et al. (2016)
HEK 293 cells	*in vitro*	5, 10, 15, 20 µM (2 hours)	DNA damage	Liu et al. (2003)
HepG2 cells	*in vitro*	0, 5, 10, 20 and 40 mM (1 hour)	Significant DNA strand breaks (20, 40 mM)	Zhou et al. (2010)
human lymphocytes using whole blood from healthy donors	*in vitro*	2.5, 5.0 and 7.5 µM (72 hours)	Formation of micronucleus	Alves et al. (2000)
wild type V79 Chinese hamster cells (MZ)	*in vitro*	0.35, 0.5, 0.65, 0.8 and 0.95 µM (24 hours)	chromosomal aberrations clastogenic activity was detectable in a very narrow dose range up to concentration of 1µM.	Alves et al. (2000)
human lymphocytes	*in vitro*	0.1, 0.3, 0.5, 1.0, 2.5, 5.0, and 7.5 µM (48 hours)	Induction of nucleoplasmic bridges (NPBs) at 5.0 and 7.5 µM	Donmez-Altuntas et al. (2013)
V79 Cells	*in vitro*	0.5 µM PAT for 3, 4.5 and 6 hours	Induction of micronuclei (MN) and nucleoplamic bridges (NPB)	Glaser and Stopper 2012
Chinese hamster V79 lung fibroblasts	*in vitro*	0, 0.5, 1, 5, 10, 50, 100 (1 hour) 0, 0.4, 0.8, 1.2, 1.6, 2, 2.4 (4 hours) 1.5 µM (6, 12, 18 and 24 hours) 0.4, 0.8, 1.2 and 1.6 µM (2 hours)	Induced DNA-DNA cross links, DNA strand breaks, and oxidative DNA modifications	Schumacher et al. (2006)
Chinese hamster V79 lung fibroblasts	*in vitro*	0-2.5 µM (24 hours)	Mutation of the HPRT gene	Schumacher et al. (2005)
HepG2 cells	*in vitro*	15 µM	p53 expression and chromosome aberrations	Ayed-Boussema (2013)
HEK293	*in vitro*	5, 30 µM (30 mins and 24 hours)	Induced DNA damage/ upregulated *EGR1* gene, regulation of *c-fos*, *fos B*, *JunB* and *gapd* not affected	Wu et al. (2005)

HEK293	*in vitro*	1,1.25, 2.5, 5,7.5 µM	DNA fragmentation, chromatin condensation, nuclear fragmentation	Wu et al. (2008)
HEK293	*in vitro*	15 µM	Formation of chromatin condensation and nuclear fragmentation	Zhang et al. (2015)
E.coli	*In vitro*	10 µg, 20 µg and 50 µg/ml (60 minutes)	DNA single-strand breaks	Lee, K.S. and Röschenthaler (1986)
skin cells from Swiss albino mice	*in vivo topical*	160 µg/100 µl acetone (6, 12, 24, 48, and 72 hours)	DNA damage	Saxena et al. (2009)